Original Article

MOLECULAR METABOLISM

# Time and metabolic state-dependent effects of GLP-1R agonists on NPY/AgRP and POMC neuronal activity *in vivo*

**Yanbin Dong [1,2,3,6], Jamie Carty [4,6], Nitsan Goldstein [4,6], Zhenyan He [5,6], Eunsang Hwang [3], Dominic Chau [3], Briana Wallace [3], Anita Kabahizi [3], Linh Lieu [3], Yunqian Peng [3], Yong Gao [2], Ling Hu [1,2,***], J. Nicholas Betley [4,**], Kevin W. Williams [3,*]**

## ABSTRACT

**Objective:** Long-acting glucagon-like peptide-1 receptor agonists (GLP-1RAs), like liraglutide and semaglutide, are viable treatments for diabetes and obesity. Liraglutide directly activates hypothalamic proopiomelanocortin (POMC) neurons while indirectly inhibiting Neuropeptide Y/Agouti-related peptide (NPY/AgRP) neurons *ex vivo*. While temporal control of GLP-1R agonist concentration as well as accessibility to tissues/cells can be achieved with relative ease *ex vivo, in vivo* this is dependent upon the pharmacokinetics of these agonists and relative penetration into structures of interest. Thus, whether liraglutide or semaglutide modifies the activity of POMC and NPY/AgRP neurons *in vivo* as well as mechanisms required for any changes in cellular activity remains undefined.

**Methods:** In order to resolve this issue, we utilized neuron-specific transgenic mouse models to examine changes in the activity of POMC and NPY/AgRP neurons after injection of either liraglutide or semaglutide (intraperitoneal - I.P. and subcutaneous - S·C.). POMC and NPY/AgRP neurons were targeted for patch-clamp electrophysiology as well as *in vivo* fiber photometry.

**Results:** We found that liraglutide and semaglutide directly activate and increase excitatory tone to POMC neurons in a time-dependent manner. This increased activity of POMC neurons required GLP-1Rs in POMC neurons as well as a downstream mixed cation channel comprised of TRPC5 subunits. We also observed an indirect upregulation of excitatory input to POMC neurons originating from glutamatergic cells that also required TRPC5 subunits. Conversely, GLP-1Ra's decreased excitatory input to and indirectly inhibited NPY/AgRP neurons through activation of K-ATP and TRPC5 channels in GABAergic neurons. Notably, the temporal activation of POMC and inhibition of NPY/AgRP neuronal activity after liraglutide or semaglutide was injected [either intraperitoneal (I.P.) or subcutaneous (S·C.)] was dependent upon the nutritional state of the animals (fed vs food-deprived).

**Conclusions:** Our results support a mechanism of liraglutide and semaglutide *in vivo* to activate POMC while inhibiting NPY/AgRP neurons, which depends upon metabolic state and mirrors the pharmacokinetic profile of these compounds *in vivo*.



**Keywords** Liraglutide and semaglutide; Long-acting glucagon-like peptide-1 receptor agonists (GLP-1RAs); TRPC5 subunit; Metabolic state-dependent effects; GLP-1R Agonists on NPY/AgRP neuron; POMC Neuronal activity

## 1. INTRODUCTION

Glucagon-like peptide-1 (GLP-1), an incretin hormone produced in L cells of the gut and in the nucleus tractus solitarius (NTS) of the hindbrain, is capable of reducing food intake, improving glucose metabolism, and lowering body weight [1—3]. Long acting GLP-1 receptor agonists (GLP-1Ra's), like liraglutide and semaglutide, have been developed and are effective therapeutic agents in the treatment of diabetes and chronic weight management [4—6]. GLP-1Ras are located in the periphery as well as the central nervous system (CNS) and contribute to a distributed network of neurons responsible for its metabolic benefits.

[1]Institute of Gastroenterology, Guangzhou University of Chinese Medicine, Guangzhou, Guangdong, China [2]Science and Technology Innovation Center, Guangzhou University of Chinese Medicine, Guangzhou, Guangdong, China [3]Center for Hypothalamic Research, Department of Internal Medicine, the University of Texas Southwestern Medical Center at Dallas, Dallas, TX, USA [4]Department of Biology, University of Pennsylvania, Philadelphia, PA, 19104, USA [5]Department of Neurosurgery, the affiliated Tumor Hospital of Zhengzhou University, Zhengzhou, Henan, 450008, China

[6] These authors are co-first authors.

*Corresponding author. University of Texas Southwestern Medical Center at Dallas, 5323 Harry Hines Boulevard, Dallas, TX, 75390-9077, USA. E-mail: kevin.williams@utsouthwestern.edu (K.W. Williams).

***Corresponding author. Institute of Gastroenterology, Guangzhou University of Chinese Medicine, Guangzhou, Guangdong, China. E-mail: drhuling@163.com (L. Hu).

**Corresponding author. E-mail: jnbetley@sas.upenn.edu (J.N. Betley).

Received September 1, 2021 • Revision received September 30, 2021 • Accepted October 2, 2021 • Available online 6 October 2021

https://doi.org/10.1016/j.molmet.2021.101352

 

Within the hypothalamic arcuate nucleus, activation of Proopiomelanocortin (POMC) neurons or an increased release of the biologically active peptide alpha-MSH (α-MSH) is associated with a reduction in food intake, increased energy expenditure, and improved glucose control [7—10]. In contrast, increased activity of NPY/AgRP neurons enhances food intake and decreases energy expenditure, thus impairing glucose metabolism [8,9,11,12]. Importantly, GLP-1RAs target and act directly on neurons within the arcuate nucleus, including POMC neurons, at least in partly reducing body weight and lower blood glucose levels [13—15]. The metabolic improvements observed in response to GLP-1R agonists appear to require cellular mechanisms (i.e. G-protein signalling and TRPC5 subunits) which result in the activation of POMC neurons [14,16]. Besides activating arcuate POMC neurons, GLP-1Ras indirectly inhibit neuropeptide-Y/agouti-related protein (NPY/AgRP) cells, via TRPC5 subunits and Katp channels [14,15]. Together these data highlight an important role of central melanocortin activity in GLP-1 dependent regulation of energy balance.

While a mechanism of action for GLP-1R signalling in arcuate POMC and NPY/AgRP neurons has been suggested, its *in vivo* occurrence remains undefined. Changes in cellular activity in response to GLP-1 and GLP-1R agonists were reported in response to acute administration in an *ex-vivo* preparation [14,15,17]. Recent work using in-vivo fibre photometry suggest that intraperitoneal (I.P.) injection of GLP-1 or GLP-1R agonists fails to alter arcuate AgRP activity *in vivo* within 30 min of injection [18,19]. However, GLP-1 is rapidly degraded (within minutes) which may preclude peripheral native or injected GLP-1 from reaching the arcuate nucleus [5,20,21]. This timeline does not match the kinetics of long-acting GLP-1R agonists measured in the blood of rodents and humans, with peak concentrations of liraglutide occurring 4—12 h after injection and returning to baseline 30—48 h after injection [22—27]. In the current study, we hypothesized that changes in the cellular activity of arcuate POMC and NPY/AgRP neurons occur in a manner temporally associated with the pharmacokinetic properties of the long-acting GLP-1R agonists (liraglutide and semaglutide). To confirm this hypothesis and examine underlying cellular mechanisms in the changes in neural activity, we utilized transgenic and Cre-Lox technology to identify and target NPY/AgRP and POMC neurons for electrophysiological recordings up to 48 h following injection of GLP-1R agonists (liraglutide and semaglutide). GLP-1R dependent effects were assessed on intrinsic membrane properties and synaptic responses of POMC and NPY/AgRP neurons. We also utilized *in vivo* fiber photometry over similar periods.

## 2. METHODS

### 2.1. Animals

Male (6—24 weeks old) pathogen-free mice were used for all experiments. All mice were housed under standard laboratory conditions (12 h on/off cycle; lights on at 7:00 am) and the temperature-controlled environment with food and water available ad libitum. All experiments were performed in accordance with the guidelines by the National Institutes of Health Guide for the Care and Use of Laboratory Animals and approved by The University of Texas Institutional Animal Care and Use Committee.

To identify POMC and NPY neurons for electrophysiological recordings, POMC- or NPY-humanized Renilla green fluorescent protein (hrGFP) mice were utilized (Parton et al., 2007 [28]; van den Pol et al., 2009 [29]). In some experiments, POMC and NPY neurons were targeted in mice globally deficient for TRPC5 subunits by mating POMC-hrGFP and NPY-hrGFP mice with TRPC5 KO mice [30,31]. POMC-cre$^{ERT2}$ mice [32] were separately mated with TRPC5$^{lox/lox}$::tdTomato [30] or GLP-1 R$^{lox/lox}$::tdtomato mice [33] to generate mice with selective deficiency of TRPC5 or GLP-1 receptor in all POMC neurons (POMC-cre$^{ERT2}$:TRPC5$^{lox/lox}$:tdTomato mice, POMC-cre$^{ERT2}$:GLP-1R$^{lox/lox}$:tdTomato).

### 2.2. Tamoxifen treatment to induce adult-onset ablation of TRPC5 or GLP-1R in POMC neurons

Tamoxifen (Sigma—Aldrich, 15 mg/ml) dissolved in corn oil (Sigma) was administered I.P. by body weight (approx. 200 μl/day) to 8-week-old male POMC-cre$^{ERT2}$:TRPC5$^{lox/lox}$:tdTomato mice or POMC-cre$^{ERT2}$:GLP-1R$^{lox/lox}$:tdTomato mice. Moist food was provided after the injection of tamoxifen. After 2 weeks of injection, mice were used for electrophysiology and molecular medicine studies.

### 2.3. Electrophysiology studies

#### 2.3.1. Slice preparation

Brain slices were prepared from male mice as previously described [14,17,30,34—36]. Briefly, male mice were deeply anesthetized with I.P. injection of 7% chloral hydrate and transcardially perfused with a modified ice-cold artificial cerebrospinal fluid (ACSF) (described below). The mice were then decapitated, their entire brain was removed, and immediately submerged in ice-cold, carbogen-saturated (95% O2 and 5% CO2) ACSF (126 mM NaCl, 2.8 mM KCl, 1.2 mM $MgCl_2$, 2.5 mM $CaCl_2$, 1.25 mM $NaH_2PO_4$, 26 mM $NaHCO_3$, and 5 mM glucose). Coronal sections (250 mm) were cut with a Leica VT1000S Vibratome and then incubated in oxygenated ACSF at room temperature for at least 1 h before recording. The slices were bathed in oxygenated ACSF (32 °C- 34 °C) at a flow rate of ∼2 ml/min. All brain slices were prepared using oxygenated ACSF, as described above.

#### 2.3.2. Whole-cell recording

The pipette solution for whole-cell recording was modified to include an intracellular dye (Alexa Fluor 350 hydrazide dye) for whole-cell recording: 120 mM K-gluconate, 10 mM KCl, 10 mM HEPES, 5 mM EGTA, 1 mM $CaCl_2$, 1 mM $MgCl_2$, and 2 mM MgATP, 0.03 mM Alexa Fluor 350 hydrazide dye (pH 7.3). Epifluorescence was used to target fluorescent cells, at which time the light source was switched to infrared differential interference contrast imaging to obtain the whole-cell recording (Zeiss Axioskop FS2 Plus equipped with a fixed stage and a QuantEM:512SC electron-multiplying charge-coupled device camera). Electrophysiological signals were recorded using an Axopatch 700B amplifier (Molecular Devices); low-pass filtered at 2—5 kHz and analyzed offline on a PC with patch-clamp (pCLAMP) electrophysiology data acquisition and analysis program (Molecular Devices). Membrane potentials and firing rates were determined from POMC and NPY neurons in brain slices. Recording electrodes showed resistances of 2.5—5 MΩ when filled with the K-gluconate internal solution. Input resistance (IR) was assessed by measuring voltage deflection at the end of the response to a hyperpolarizing rectangular current pulse step (500 ms of −10 to −50 pA).

The neurons were voltage-clamped at −70 mV (for excitatory postsynaptic currents) and −15 mV (for inhibitory postsynaptic currents). Frequency and peak amplitude were measured by using the Mini Analysis program (Synaptosoft, Inc.).

### 2.4. Drugs

Drug working concentrations and stock preparation were as follows: liraglutide (1 μM for incubation, 300ug/Kg for injection, Novo Nordisk), semaglutide (30 nmol/kg for injection, Ozempic), picrotoxin (50 μM for

 

recording, dissolved in dimethyl sulfoxide, Sigma Aldrich), diazoxide (200 μM for recording, dissolved in dimethyl sulfoxide, Sigma Aldrich). The final concentration of dimethyl sulfoxide applied to the slice was <0.1%.

### 2.5. Animal studies

#### 2.5.1. Injection study

For the liraglutide or semaglutide injection study, age-matched male mice were injected with saline (10 ml/kg), liraglutide (300ug/Kg, Novo Nordisk), or semaglutide (30 nmol/kg for injection, Ozempic) according to the different time points.

#### 2.5.2. Exercise protocols

Motorized treadmills (Exer-6; Columbus Instruments, Columbus, OH) were used for exercise experiments. The mice were deprived of food before they were placed on the treadmills. The mice were coaxed to stay and run on the treadmill using an electric stimulus (0.25 mA × 163 V and 1 Hz) generated by a shock grid present at the treadmill base and by manually tapping their tails using a soft nylon bottle brush, as needed to enable all the mice to complete the exercise bout [34,37].

*2.5.2.1. Exercise groups.* All mice were familiarized with the treadmills for 2 days prior to the exercise bout [Prior day 1:5 min rest on the treadmill followed by 5 min at the speed of 8 m/min and then for 5 min at the speed of 10 m/min; Prior day 2: 5 min rest on the treadmill followed by 5 min at the speed of 10 m/min and then for 5 min at the speed of 12 m/min [34].

*2.5.2.2. Day 1 exercise protocol +24H injection.* On Day 1, mice were subjected to a high-intensity interval exercise (HIIE) bout to assess exercise-induced changes in electrophysiological characteristics of NPY/AgRP and POMC neurons. Mice were rested on the treadmill for 5 min prior to performing 1 h of exercise consisting of 3 × 20 min intervals (5 min at the speed of 12 m/min, followed by 10 min at the speed of 17 m/min, and then 5 min at the speed of 22 m/min), without rest between intervals. The animals were injected with either saline or liraglutide 23 h before HIIE.

#### 2.5.3. Food deprivation

All experimental procedures were conducted in accordance with the University of Pennsylvania Institutional Animal Care and Use Committee.

For 24 h of food deprivation, mice were moved to a clean cage with no access to food at the start of the light cycle (7 a.m.), 24 h before recordings began. The animals were recorded at 85–90% of original body weight. For 4 h of food deprivation, mice were moved to a clean cage with no access to food 4 h before recordings began. The animals were recorded at 97–99% of their original body weight.

#### 2.5.4. Fiber photometry

*2.5.4.1. Experimental model.* Homozygous AgRp-IRES-Cre (Jackson Labs 012,899, AgRP$^{tm1(cre)Lowl}$/J) were used for fiber photometry experiments. Mice were habituated to all experimental conditions for at least 3 days before recordings began. All mice received all experimental conditions in a counter-balanced manner and within-subjects analyses were performed.

*2.5.4.2. Viral injection and fiber optic implantation.* Stereotaxic surgeries were performed as previously described [19]. Briefly, mice were anesthetized with isoflurane (3% for induction and 1–1.5% during the surgery) and pretreated with subcutaneous injections of 5 mg/kg ketoprofen (Santa Cruz Animal Health, sc363115Rx) and 2 mg/kg bupivacaine at the incision site (Moore Medical, 52,683). Mice were placed into a stereotaxic apparatus (Stoelting, 51725D). The genetically encoded calcium indicator GCaMP6s [AAV1.Syn.-Flex.GCaMP6s.WPRE.SV40 (titer: 1.6e13 GC/ml, Addgene 100,845)] was unilaterally injected in the arcuate nucleus (ARC, 300 nL) using the following coordinates: 1.35 mm posterior to bregma, 0.25 mm lateral to the midline, and 6.15–6.3 mm ventral to the skull surface. The fiber optic ferrule was implanted 0.2 mm above the injection site and was secured to the skull using Metabond (Parkell, S380) and dental cement (Lang Dental Manufacturing, Ortho-jet BCA Liquid, B1306, and Jet Tooth Shade Powder, 143,069). The mice were given 2 weeks for recovery and viral expression before fiber photometry experiments began. Prior to experimental procedures, mice were food-deprived for 24 h and AgRP neuron responses to food presentation recorded. As previously reported (Alhadeff et al., 2019), mice only with at least a 15% ΔF/F response to a pellet of chow were used in experiments.

*2.5.4.3. Dual-wavelength fiber photometry.* Dual-wavelength fiber photometry was performed as previously described by us (Lerner, 2015 [38], [19]). Two excitation wavelengths, 470 nm and 405 nm, were simultaneously used. 470 nm excitation wavelength serves as a proxy for neural activity by exciting the calcium-dependent GCaMP6s fluorescence. Isobestic 405 nm excitation wavelength serves as a control for motion and bleaching artifacts. Fiber-coupled LEDs (Thorlabs, M470F3 for 470 nm and M405F1 for 405 nm) generated the excitation lights and real-time amplifiers (Tucker–Davis Technologies, RZ5P) modulated the excitation at 211 Hz for 470 nm and 566 Hz for 405 nm. The excitation wavelengths are passed through a series of dichroic mirrors (Doric Lenses, FMC4_AE(405)_E1(460–490)_F1(500–550)_S) and transmitted into the terminal fiber through a low auto-fluorescent patch cord (Doric Lenses, MFP_400/430/1100–0.57_1.5_FCM-MF2.5_LAF). The calcium-dependent and independent emission is collected through the same patch cord, passed through a Green Fluorescent Protein (GFP) emission filter, and focused on a femtowatt photoreceiver (Newport, Model 2151, gain set to DC LOW). The collected emission light is converted to an electrical signal using the RZ5P real-time processor controlled by Synapse software (Tucker–Davis Technologies). GCaMP6s fluorescence was set to similar levels across mice by adjusting the 470 nm and 405 nm LED power. The total power at the terminal fiber was 30–70 μW (470 nm) and 5–10 μW (405 nm). A 5-min baseline was recorded prior to food presentation and used as the baseline signal for subsequent analyses.

*2.5.4.4. Liraglutide experiments.* Mice expressing GCaMP6s in AgRP neurons were habituated to fiber photometry handling prior to experiments.

For monitoring the acute effects of Liraglutide, mice were deprived of food for 24 h. Mice were given an I.P. injection of 300 μg/kg Liraglutide (Toronto Research Chemical, L468860) or an I.P. injection of the vehicle in a counterbalanced fashion. Thereafter, 30 min, 2 h, 4 h, 12 h, and 24 h after Liraglutide injection, a 5 min baseline recording was collected in the home cage followed by the presentation of a chow pellet. AgRP neuron activity was monitored for 10 min following food delivery. Food was then removed from the cage until the next recording. Mice had ad libitum access to water during experiments.

To determine whether Liraglutide has lasting effects on *in vivo* AgRP neuron activity, ad libitum fed mice were given an I.P. injection of 300 μg/kg Liraglutide (Toronto Research Chemical, L468860) or an I.P.

 

injection of the vehicle in a counterbalanced fashion. Twenty hours after Liraglutide injection, mice were moved to a clean cage without access to food. Four hours later, a 5-min baseline recording was collected in the home cage followed by the presentation of a chow pellet. AgRP neuron activity was monitored for 10 min following food delivery.

In all, *in vivo* Liraglutide experiments, at least a week separated the counter-balanced trials to ensure that the drug had washed out and that mice returned to their original bodyweights.

### 2.6. Analysis and statistics

#### 2.6.1. Electrophysiology analysis and statics

A value of twice the mean peak-to-peak noise level for a given recording in control solutions was used as the detection limit for minimal PSC amplitude (i.e., typically 5–10 pA). For spontaneous excitatory synaptic currents and inhibitory synaptic currents (sEPSCs and sIPSCs), at least 2 min of activity was examined to identify effects on amplitude and frequency distributions. Membrane potential values were not compensated to account for junction potential (−8 mV). All graphs were plotted using GraphPad Prism 9.0 software. All figures were carried out using CorelDraw C8 (64 Bit). Data from proportions of responding cells from different groups were analyzed using unpaired a two-tailed Student's t-test or analysis of variance (ANOVA) where appropriate. Results are reported as the mean ± SEM unless indicated otherwise, as indicated in each figure legend; where n represents the number of cells studied. Significance was set at $*p < 0.05$ for all statistical measures. The data collected in each condition were obtained from ≥3 mice and from ≥9 total cells. The number of cells or mice studied for each group is shown in parentheses.

#### 2.6.2. Fiber photometry analysis and statics

Data were exported from Synapse to MATLAB (Mathworks) using a script provided by Tucker–Davis Technologies. Custom MATLAB scripts were used to down-sample the data to 1Hz and normalize both the 470 nm and 405 nm data. ΔF/F was calculated as $(F\text{-}F_{baseline})/F_{baseline}$, with $F_{baseline}$ being the median of the 5-min pre-stimulus signal. Mean ΔF/F was calculated by integrating ΔF/F over some time and dividing by the integration time. Minimum ΔF/F was calculated using the 10 s mean ΔF/F for each mouse at the average minimum of each recording. All data are expressed as mean ± SEM in the figures. Paired two-tailed t-tests and repeated measures two-way ANOVAs were used to make comparisons where appropriate using GraphPad Prism version 9.

N represents the number of animals studied. ns $> 0.05$, unpaired t-test and post-hoc comparison: $*p < 0.05$, $**p < 0.01$.

## 3. RESULTS

### 3.1. Extended liraglutide administration activates POMC and inhibits NPY/AgRP neurons ex-vivo

Previous electrophysiological studies have remained limited to *ex vivo* measurement of acute GLP-1Ras administration to arcuate POMC or NPY/AgRP neurons [14,15,17]. While this results in a rapid change in the cellular activity of both POMC and NPY/AgRP neurons, the time required for long-acting GLP-1Ras to maximally alter POMC or NPY/AgRP neuronal activity **in vivo** remains unclear. In the first step toward understanding the effects of GLP-1Ra on the activity of arcuate POMC and NPY/AgRP neurons *in vivo*, we examined the chronic effects of GLP-1Ra *ex vivo*. We incubated hypothalamic slices containing arcuate POMC and NPY/AgRP neurons with ACSF containing liraglutide (1 μM) for up to 2 h. After incubation, the slices were moved to the recording chamber; POMC or NPY/AgRP neurons were targeted for whole-cell patch-clamp electrophysiological recordings. When $K^+$ was used as the major cation in the recording pipette, arcuate NPY/AgRP neurons incubated with saline (n = 21) had a resting membrane potential (RMP) of −38.5 ± 1.0 mV and a mean IR of 1.6 ± 0.1 MΩ. Similar to previous reports on the acute effects of liraglutide on arcuate NPY neurons [14,15], incubation of NPY neurons with liraglutide (1 μM, for 2 h) resulted in a hyperpolarized RMP concomitant with a decrease in action potential frequency (APF) and increased inhibitory synaptic input to arcuate NPY neurons (Figure 1). We also observed a decrease in the frequency of excitatory input to NPY neurons following incubation with liraglutide, which may contribute, to an enhanced inhibition (Figure 1). Arcuate POMC neurons incubated with saline (n = 14) had an RMP of −46.1 ± 1.1 mV and a mean IR of 1.4 ± 0.1 MΩ. Similar to the acute effects of liraglutide on arcuate POMC neurons, incubation of POMC neurons with liraglutide (1 μM, for 2 h) resulted in a depolarized RMP concomitant with an increase in APF and increased excitatory synaptic input to arcuate POMC neurons (Figure 2). We also observed an increase in the frequency of inhibitory input to POMC neurons following incubation with liraglutide (Figure 2). Together these data confirm the hypothesis that chronic exposure to GLP-1RA changes the electrophysiological properties of POMC and NPY/AgRP neurons, persisting well beyond the removal of the GLP-1RA. We next examined the effects of injecting GLP-1RA into awake and behaving mice on the electrophysiological properties of NPY/AgRP and POMC neurons in a slice preparation *ex vivo*.

### 3.2. Liraglutide and semaglutide inhibit NPY/AgRP neurons in-vivo in a time-dependent manner

To date, no in-depth analyses on the time-dependent effects of GLP-1RA on arcuate NPY/AgRP and POMC neuronal activity have been conducted in brain slices or *in vivo*. In order to understand how liraglutide regulates the activity of NPY/AgRP neurons in the arcuate, we first performed whole-cell patch-clamp recordings on 206 arcuate NPY neurons *ex vivo* at different time points (30 min, 2 h, 12 h, 24 h, and 48 h) after an i.p. Injection of saline or liraglutide (300 μg/kg, Figure 3 A–G). We hypothesize this as a viable method to investigate *in vivo* effects of GLP-1RAs on the cellular properties of NPY/AgRP neurons because we have previously demonstrated that the effects of GLP-1RA on both NPY/AgRP and POMC neurons persist after removal of the GLP-1Ra (Figures 1 and 2). We found that NPY neurons were hyperpolarized 12 and 24 h after injection of liraglutide (300 μg/kg, I.P., Figure 3 A, Figure S5 A). When compared to values of NPY neurons from saline-injected mice, the hyperpolarized membrane potential observed in NPY neurons from mice 24 h after injection with liraglutide was concomitant with decreased APF (Figures 3 B, S5 A). The average IR was also decreased 24 h after injection of liraglutide (300 μg/kg, I.P., Figure 3C).

The inhibition of arcuate NPY neurons in response to acute [14,15] and chronic exposure to liraglutide have been suggested to require increased inhibitory synaptic activity (Figure 1M–P). An analogous increase in IPSC frequency was observed in NPY neurons 12 and 24 h after injection of liraglutide (300 μg/kg, I.P., at 12 and 24 h, Figures 3 F, S5 C), while the amplitude of sIPSCs remained unchanged (Figure 3 G, S5 C). Similar to chronic exposure, liraglutide (300 μg/kg, I.P., at 24 h) decreased the frequency of excitatory input to NPY neurons, independent of changes in amplitude (Figure 3 D-E, S5 B). Comparable effects were observed after S.C. injection of liraglutide (300 μg/kg) or Semaglutide (30 nmol/kg, Figure S1A–G).

 

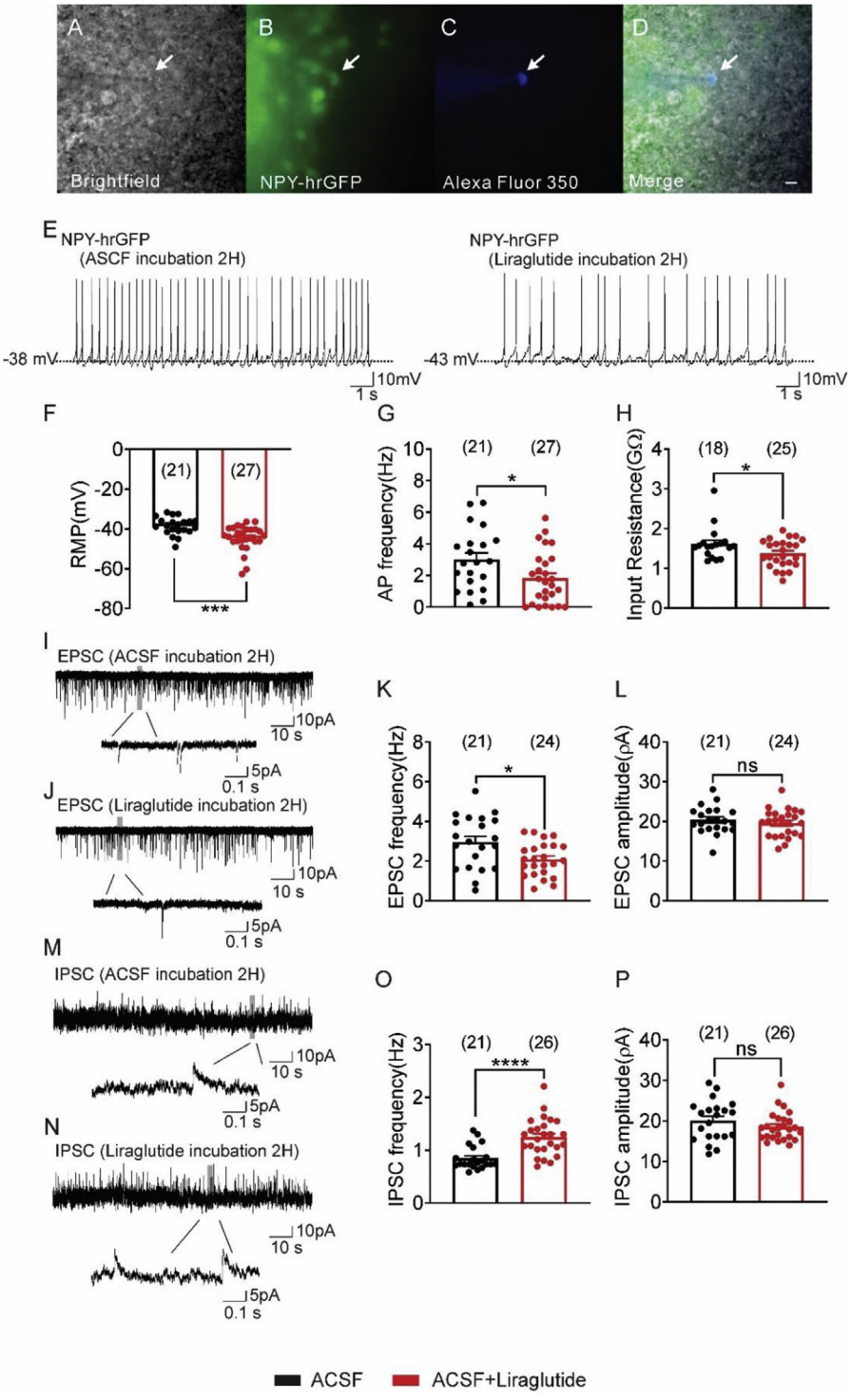


**Figure 1:** Incubation (2 h) of hypothalamic slices containing the arcuate with liraglutide inhibits arcuate NPY neurons from ad *libitum* fed animals. (A–D) NPY-hrGFP neuron: (A) Brightfield illumination of an NPY-hrGFP neuron. (B) Same neuron under FITC (hrGFP). (C) The image shows the complete dialysis of Alexa Fluor 350 from the intracellular pipette. (D) Merged image of targeted NPY-hrGFP neuron. Arrow indicates the targeted cell, Scale bar = 50 μm. (E) Current-clamp recording of an NPY-hrGFP neuron shows the resting membrane potential 2H after incubation with either ACSF or ACSF + liraglutide (1 μM). (F–H) Histogram demonstrating the average resting membrane potential of NPY-hrGFP neurons (F), action potential frequency (G), and input resistance (H) 2 h after incubation with either ACSF or ACSF + liraglutide. (I–J) Voltage clamp recording (Vm = −70 mV) of sEPSCs from NPY-hrGFP neurons 2H after incubation with ACSF (I) or ACSF + liraglutide (J). (K–L) Plots indicating the decreased sEPSCs frequency (Hz) and independent of changes in amplitude (pA) in NPY-hrGFP neurons 2H after incubation with liraglutide compared with control ACSF group. (M–N) Voltage clamp recording (Vm = −15 mV) of sIPSCs from NPY-hrGFP neurons 2H after incubation with ACSF (M) or ACSF + liraglutide (N). (O–P) Plots showing an increased sIPSCs frequency (Hz) and no change in amplitude (pA) in arcuate NPY-hrGFP neurons 2 h after incubation with liraglutide compared with the control group (black bar: ACSF; red bar: ACSF + liraglutide). Data are taken from male mice and are expressed as mean ± SEM. *$p < 0.05$, ***$p < 0.001$, ****$p < 0.0001$, unpaired t-test compared to controls. The number of neurons studied for each group is in parentheses.

 

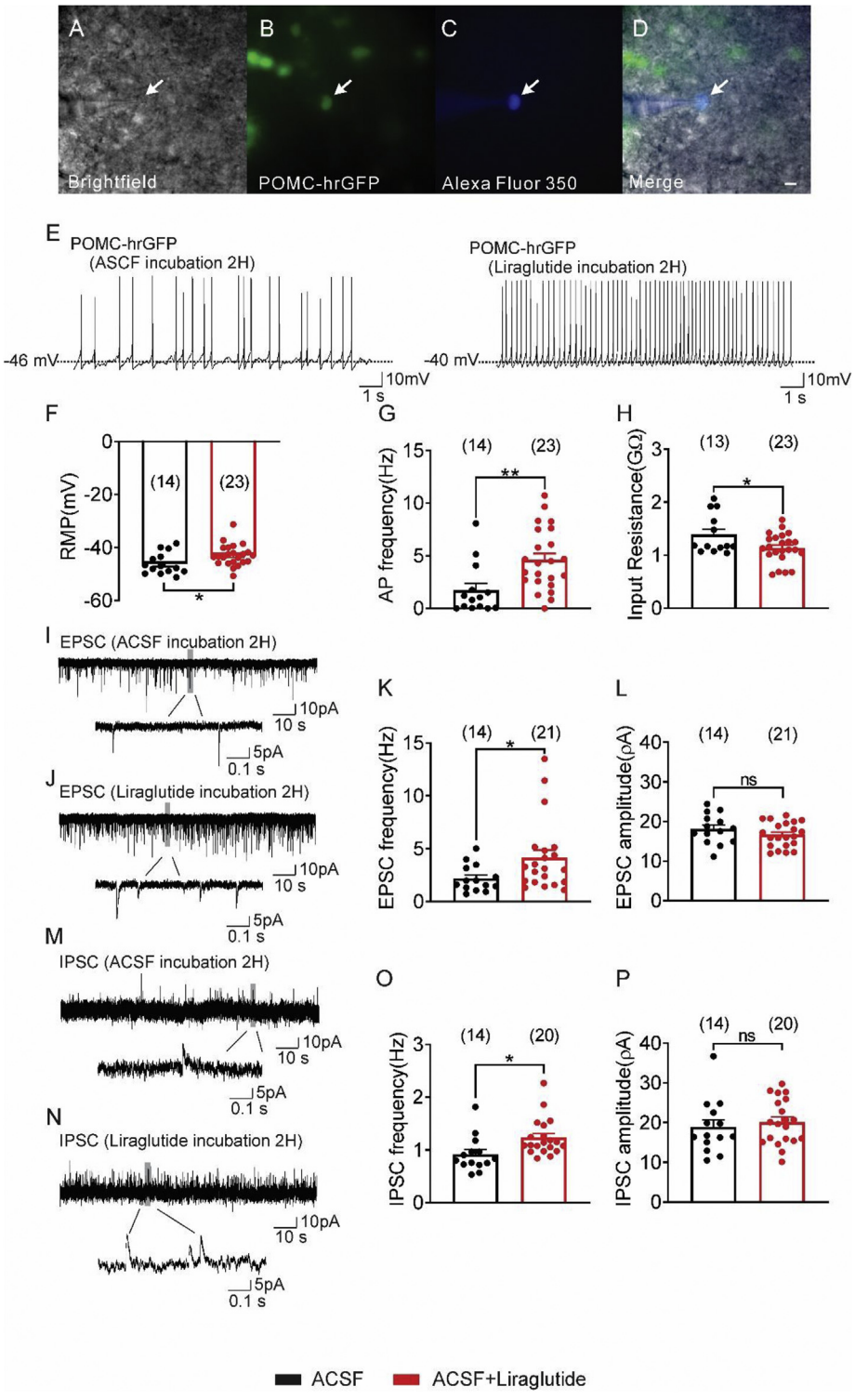


**Figure 2:** Incubation (2 h) of hypothalamic slices containing the arcuate with liraglutide activates arcuate POMC neurons from ad *libitum* fed animals. (A–D) POMC-hrGFP neuron: (A) Brightfield illumination of POMC-hrGFP neuron. (B) Same neuron under FITC (hrGFP). (C) The image shows the complete dialysis of Alexa Fluor 350 from the intracellular pipette. (D) Merged image of targeted POMC-hrGFP neuron. Arrow indicates the targeted cell, Scale bar = 50 μm. (E) Current-clamp recording of a POMC-hrGFP neuron shows the resting membrane potential 2 h after incubation with ACSF or ACSF + liraglutide (1 μM). (F–H) Histogram demonstrating the average resting membrane potential of POMC-hrGFP neurons (F), action potential frequency (G), and input resistance (H) 2 h after incubation with ACSF or ACSF + liraglutide. (I–J) Voltage clamp recording (Vm = −70 mV) of sEPSCs from POMC-hrGFP neurons 2 h after incubation with ACSF (I) or ACSF + liraglutide (J). (K–L) Plots demonstrating an increased sEPSCs frequency (Hz) and independent of changes in amplitude (pA) in arcuate POMC-hrGFP neurons 2 h after incubation with liraglutide compared with the control group. (M–N) Voltage clamp recording (Vm = −15 mV) of sIPSCs in POMC-hrGFP neurons 2 h after incubation with ACSF (M) or ACSF + liraglutide (N). (O–P) Plots indicating an increased sIPSCs frequency (Hz) and no change in amplitude (pA) in arcuate POMC-hrGFP neurons 2 h after incubation with liraglutide compared with the control group (black bar: ACSF; red bar: ACSF + liraglutide). Data are from male mice and are expressed as mean ± SEM. *p < 0.05, **p < 0.01, unpaired t-test compared to controls. The number of neurons studied for each group is in parentheses.

 

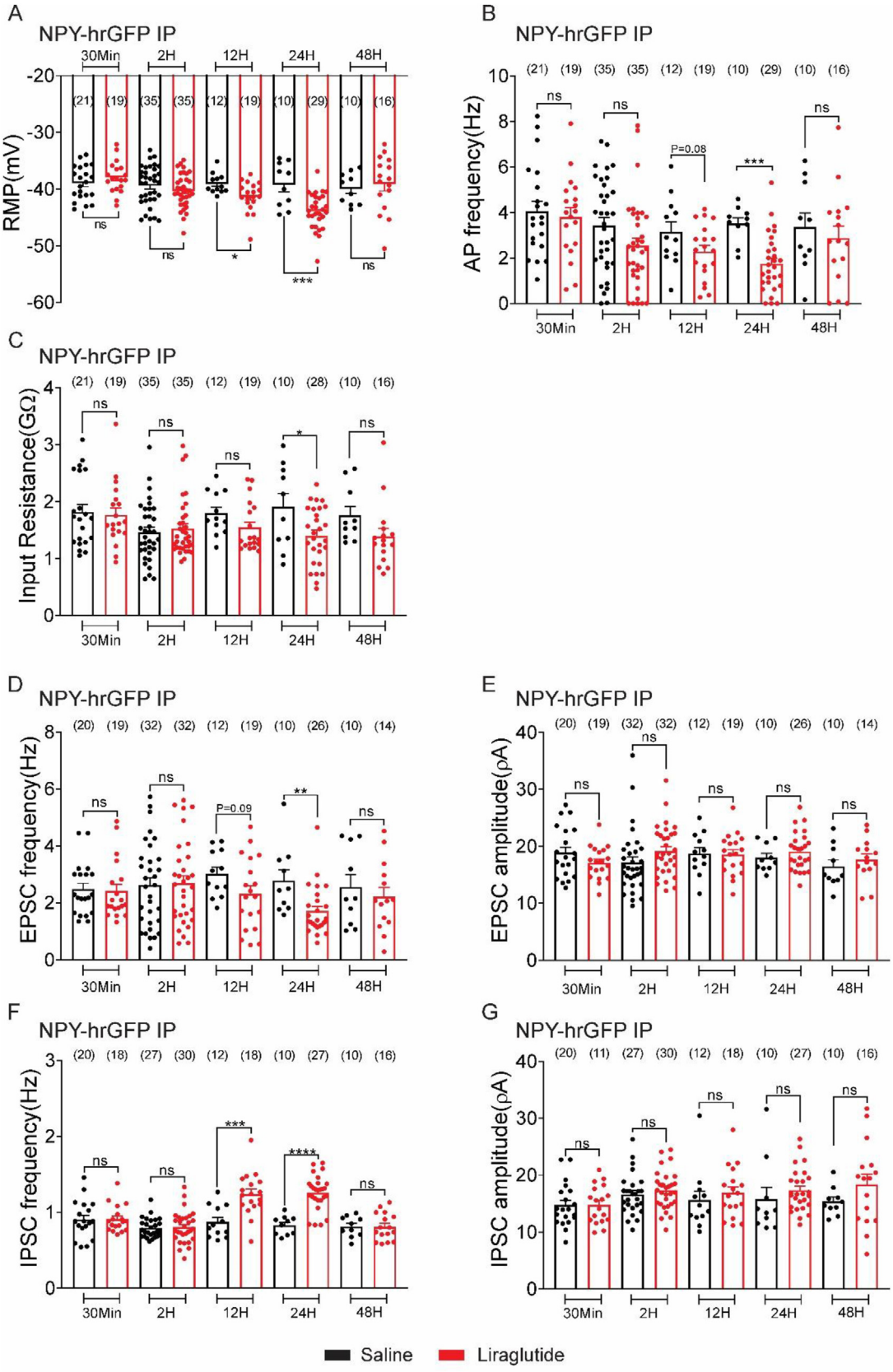


**Figure 3:** Intraperitoneal (I.P.) injection of liraglutide inhibits arcuate NPY neurons from ad *libitum* fed mice. (A–G) Histogram demonstrating the average resting membrane potential (A), action potential frequency (B), input resistance (C), sEPSCs frequency (D), sEPSCs amplitude (E), sIPSCs frequency (F), and sIPSCs amplitude (G) of NPY-hrGFP neurons 30 min, 2 h, 12 h, 24 h or 48 h after injection saline or liraglutide (black bar: saline; red bar: liraglutide, 300 μg/kg, I.P.). Data are from male mice and are expressed as mean ± SEM. *$p < 0.05$, **$p < 0.01$, ***$p < 0.001$, ****$p < 0.0001$, unpaired t test compared to controls. The number of neurons studied for each group is in parentheses.

 

### 3.3. Temporal activation of arcuate POMC neurons by liraglutide and semaglutide *in vivo*

Similarly, whole-cell pCLAMP recordings were done in 234 arcuate POMC neurons from POMC-hrGFP mice at different time points (30 min, 2 h, 12 h, 24 h, and 48 h) after an I.P. injection of saline or liraglutide (Figure 4 A—G). POMC neurons were depolarized 12 and 24 h post injection of liraglutide (300 μg/kg, I.P., Figures 4 A, S5 D). When compared to values of POMC neurons from saline-injected mice, the depolarized membrane potential observed in POMC neurons from mice 12 and 24 h after injection with liraglutide was concomitant with an increased APF (300 μg/kg, I.P., Figures 4 B, S5 D). The average IR was also decreased 24 h after injection of liraglutide (Figure 4 C).

Acute and chronic exposure to liraglutide results in an increase in excitatory synaptic input to POMC neurons (Figure 2I—L). An analogous increase in excitatory neurotransmission was observed 24 h after injection of liraglutide (300 μg/kg, I.P., at 24 h), while the amplitude of sEPSCs remained unchanged (Figure 4 D-E, S5 E). Similar to chronic exposure, liraglutide (300 μg/kg, I.P., at 12 and 24 h) increased the frequency of inhibitory input to POMC neurons (Figure 2I—L), independent of changes in amplitude (Figure 4 F-G, S5 F). Comparable effects were observed after subcutaneous (S·C.) injection of liraglutide (300 μg/kg) or Semaglutide (30 nmol/kg, Figure S2A—G).

### 3.4. The liraglutide-induced activation of POMC neurons *in vivo* requires GLP-1Rs in POMC neurons

In order to investigate the requirement of GLP-1Rs in the activation of arcuate POMC neurons, whole-cell patch-clamp recordings were performed on 33 arcuate POMC neurons selectively deficient for GLP-1Rs from POMC-Cre$^{ERT2}$:GLP-1R$^{lox/lox}$:tdtomato mice. Neurons were targeted 24 h after injection of saline or liraglutide (I.P.), which mirrored the time point at which we previously observed the maximum effect of liraglutide on POMC neuronal activity (Figure 4). Following injection of saline (I.P., after 24 h), arcuate POMC neurons deficient for GLP-1Rs had an average RMP of $-46.3 \pm 0.9$ mV, $n = 14$, a mean APF of $1.1 \pm 0.3$ Hz, $n = 14$, a mean IR of $1.1 \pm 0.1$ GΩ, $n = 14$ (Figure 5 A-C, S6 A). When compared to values obtained from arcuate POMC neurons 24 h after injection of liraglutide; liraglutide failed to alter the RMP, APF and IR (300 μg/kg, after 24 h, I.P.; RMP $= -45.2 \pm 0.8$ mV, $p > 0.05$, $n = 19$; APF $= 0.8 \pm 0.2$ Hz, $p > 0.05$, $n = 19$; IR $= 1.0 \pm 0.1$ GΩ, $p > 0.05$, $n = 19$, Figure 5 A-C, S6 A).

While deficiency of GLP-1Rs in POMC neurons abrogated the effects of liraglutide on post-synaptic cellular activity, the liraglutide-induced effects on presynaptic inputs remained intact. In particular, the frequency of sEPSCs for arcuate POMC neurons 24 h after an I.P. injection of saline was: $2.1 \pm 0.3$ Hz, $n = 14$ (Figures 5 D, S6 B). Similar to acute [14,15,17], chronic exposure, and injection of liraglutide in control mice; the sEPSCs frequency was increased 24 h after injection of liraglutide in mice deficient for GLP-1Rs in POMC neurons (300 μg/kg, I.P., at 24 h; $3.3 \pm 0.3$ Hz, $p < 0.05$, $n = 19$, Figures 5 D, S6 B), while the amplitude of sEPSCs remained unchanged (Figure 5 E). The frequency of sIPSCs was also increased 24 h after injection of liraglutide in mice deficient for GLP-1Rs in POMC neurons (I.P., at 24 h; for saline: $1.0 \pm 0.1$ Hz, $n = 12$; for liraglutide: $1.6 \pm 0.2$ Hz, $p < 0.05$, $n = 19$, Figure 5 F, S6 C), while the amplitude of sIPSCs remained unchanged (Figure 5 G).

### 3.5. In vivo effects of liraglutide on POMC activity requires TPRC5 channels in POMC neurons independent of presynaptic TRPC5 expression

On the basis of a previous work on the acute effects of Liraglutide on arcuate POMC neurons [14], we hypothesized that TRPC5 subunits may be required for *in vivo* activation of arcuate POMC neurons by GLP-1Ras. In order to confirm this hypothesis, we first targeted POMC neurons from mice globally deficient for TRPC5 subunits [POMC-hrGFP:TRPC5KO [30]] 24 h after injection of saline or liraglutide (300 μg/kg, I.P.; Figure 5H—N). Arcuate POMC neurons from mice injected with saline showed an average RMP of $-44.1 \pm 1.1$ mV, $n = 26$, a mean APF of $1.7 \pm 0.4$ Hz, $n = 26$, a mean IR of $1.2 \pm 0.1$ GΩ, $n = 26$ (Figure 5 H-J, S6 D). Liraglutide failed to alter all of these properties in POMC neurons from mice globally deficient for TRPC5 subunits (RMP $= -43.6 \pm 1.6$ mV, $p > 0.05$, $n = 15$; APF $= 1.8 \pm 0.5$ Hz, $p > 0.05$, $n = 15$; IR $= 1.3 \pm 0.1$ GΩ, $p > 0.05$, $n = 15$, Figure 5 H-J, Figure S6 D). Notably, the frequency of excitatory and inhibitory input to POMC neurons remained unchanged in response to liraglutide in mice globally deficient for TRPC5 subunits (sEPSCs: 24 h after saline, I.P.: $1.8 \pm 0.2$ Hz, $n = 25$; 24 h after liraglutide, I.P.: sEPSCs $= 1.9 \pm 0.3$ Hz, $p > 0.05$, $n = 15$; sIPSCs: 24 h after saline, I.P.: $0.7 \pm 0.1$ Hz, $n = 22$, 24 h after liraglutide, I.P.: $0.7 \pm 0.1$ Hz, $p > 0.05$, $n = 15$, Figure 5 K—N, S6 E,F). Thus, in addition to a requirement in stimulating postsynaptic POMC activity, these data extend the role of TRPC5 subunits downstream of GLP-1Rs to activate both excitatory and inhibitory presynaptic inputs of arcuate POMC neurons.

Next, we investigated the requirement of TRPC5 subunits in POMC neurons alone to contribute to the GLP-1Ra dependent changes in the post-synaptic and pre-synaptic activity of POMC neurons. POMC neurons from mice selectively deficient for TRPC5 subunits only in POMC neurons (using POMC-cre$^{ERT2}$:TRPC5$^{lox/lox}$:tdtomato) were targeted for electrophysiological recordings 24 h after injection with saline or Liraglutide (300 μg/kg, I.P.). Arcuate POMC neurons selectively deficient for TRPC5 subunits showed an average RMP of $-43.4 \pm 1.5$ mV, $n = 17$; a mean APF of $1.7 \pm 0.3$ Hz, $n = 17$, a mean IR of $1.0 \pm 0.1$ GΩ, $n = 17$ (Figure 5 O-Q, S6 G). Similar to data obtained from mice globally deficient for TRPC5 subunits (Figure 5H—J), liraglutide could not alter these properties in POMC neurons selectively deficient for TRPC5 (RMP $= -43.4 \pm 1.2$ mV, $p > 0.05$, $n = 24$; APF $= 1.8 \pm 0.3$ Hz, $p > 0.05$, $n = 24$; IR $= 1.0 \pm 0.1$ GΩ, $p > 0.05$, $n = 24$, Figure 5 O-Q, S6 G). The frequency of excitatory and inhibitory inputs to POMC neurons remained increased in response to liraglutide in mice selectively deficient for TRPC5 subunits in POMC neurons (sEPSCs: 24 h after saline, I.P.: $3.1 \pm 0.4$ Hz, $n = 14$; 24 h after liraglutide, I.P.: $4.5 \pm 0.4$ Hz, $p < 0.05$, $n = 19$; frequency of sIPSCs: 24 h after saline, I.P.: $1.1 \pm 0.2$ Hz, $n = 15$; 24 h after liraglutide, I.P.: $1.8 \pm 0.3$ Hz, $p < 0.05$, $n = 19$; Figure 5 R—U, S6 H,I). These data suggest that the GLP-1Ra induced increase in synaptic activity to POMC neurons is not required for the GLP-1Ra dependent activation of arcuate POMC neurons.

### 3.6. In vivo effects of liraglutide on NPY/AgRP activity requires TRPC5 and KATP channels in presynaptic GABAergic neurons

On the basis of a previous work on the acute effects of Liraglutide on arcuate NPY/AgRP neurons [14], we hypothesized that TRPC5 subunits and KATP channels may be required for an *in vivo* increase in inhibitory input to arcuate NPY/AgRP neurons by GLP-1Ras. In order to assess this activity, we first targeted NPY neurons from mice globally deficient for TRPC5 subunits (NPY-hrGFP:TRPC5KO) 24 h after injection of saline or liraglutide (300 μg/kg, I.P.; Figure 6 A-D, S7 A,B). As expected, the liraglutide-induced increase in inhibitory synaptic activity persisted in mice globally deficient for TRPC5 channels (sIPSCs: 24 h after saline, I.P.: $0.6 \pm 0.1$ Hz, $n = 18$; 24 h after liraglutide, I.P.: sIPSCs: $1.2 \pm 0.1$ Hz, $p < 0.0001$, $n = 15$, Figures 6 A, S7 A). In order to assess the dual requirement of TRPC5 subunits and KATP channels, we

 

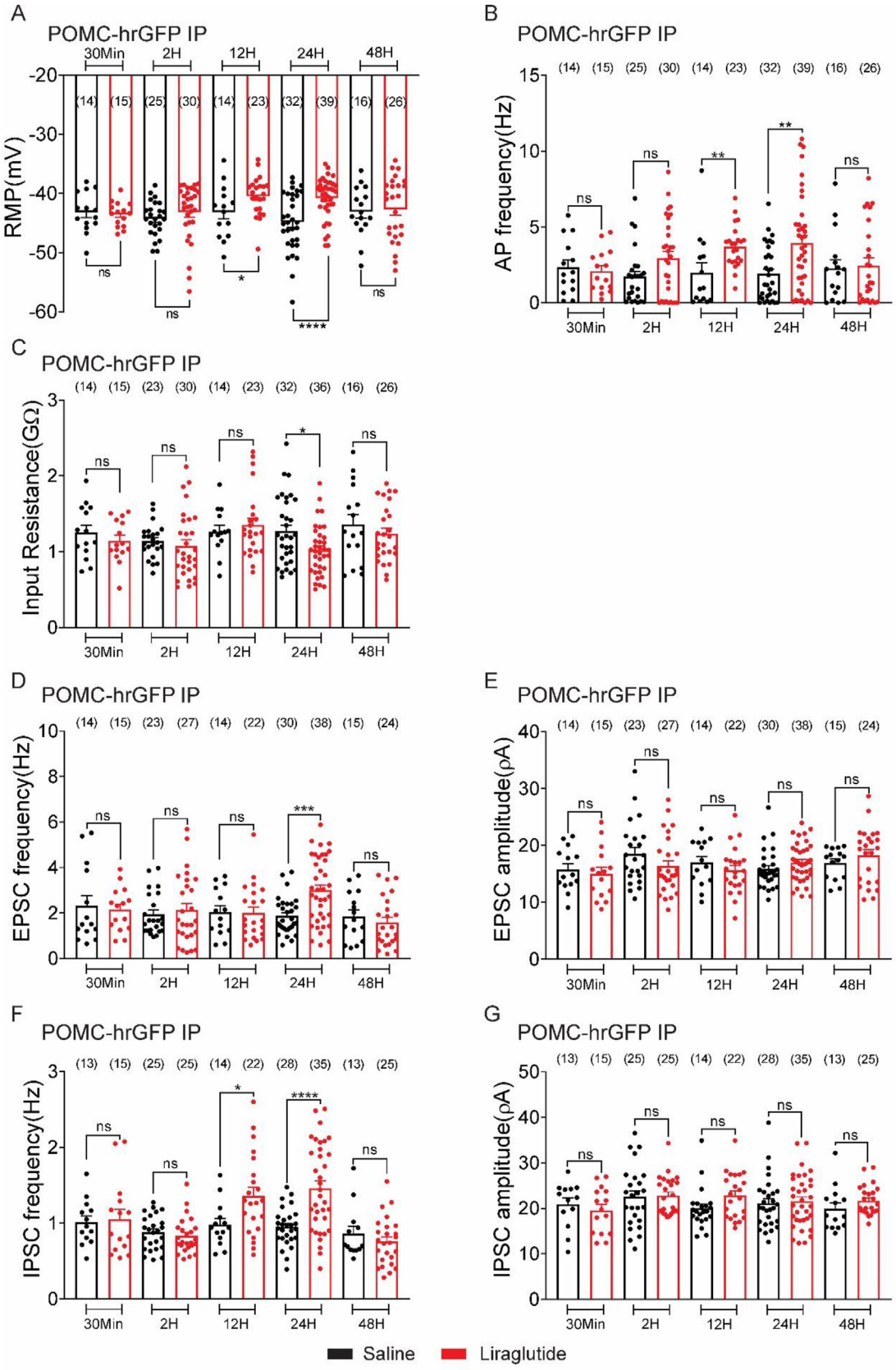


**Figure 4:** Intraperitoneal (i.p.) injection of liraglutide activates arcuate POMC neurons from ad libitum fed mice. (A–G) Histogram demonstrating the average resting membrane potential (A), action potential frequency (B), input resistance (C), sEPSCs frequency (D), sEPSCs amplitude (E), sIPSCs frequency (F), and sIPSCs amplitude (G) of POMC-hrGFP neurons 30 Min, 2 h, 12 h, 24 h or 48 h after injection saline or liraglutide (black bar: saline; red bar: liraglutide, 300 μg/kg, I.P.). Data are from male mice and are expressed as mean ± SEM. *$p < 0.05$, **$p < 0.01$, ***$p < 0.001$, ****$p < 0.0001$, unpaired t test compared to controls. The number of neurons studied for each group is in parentheses.

 

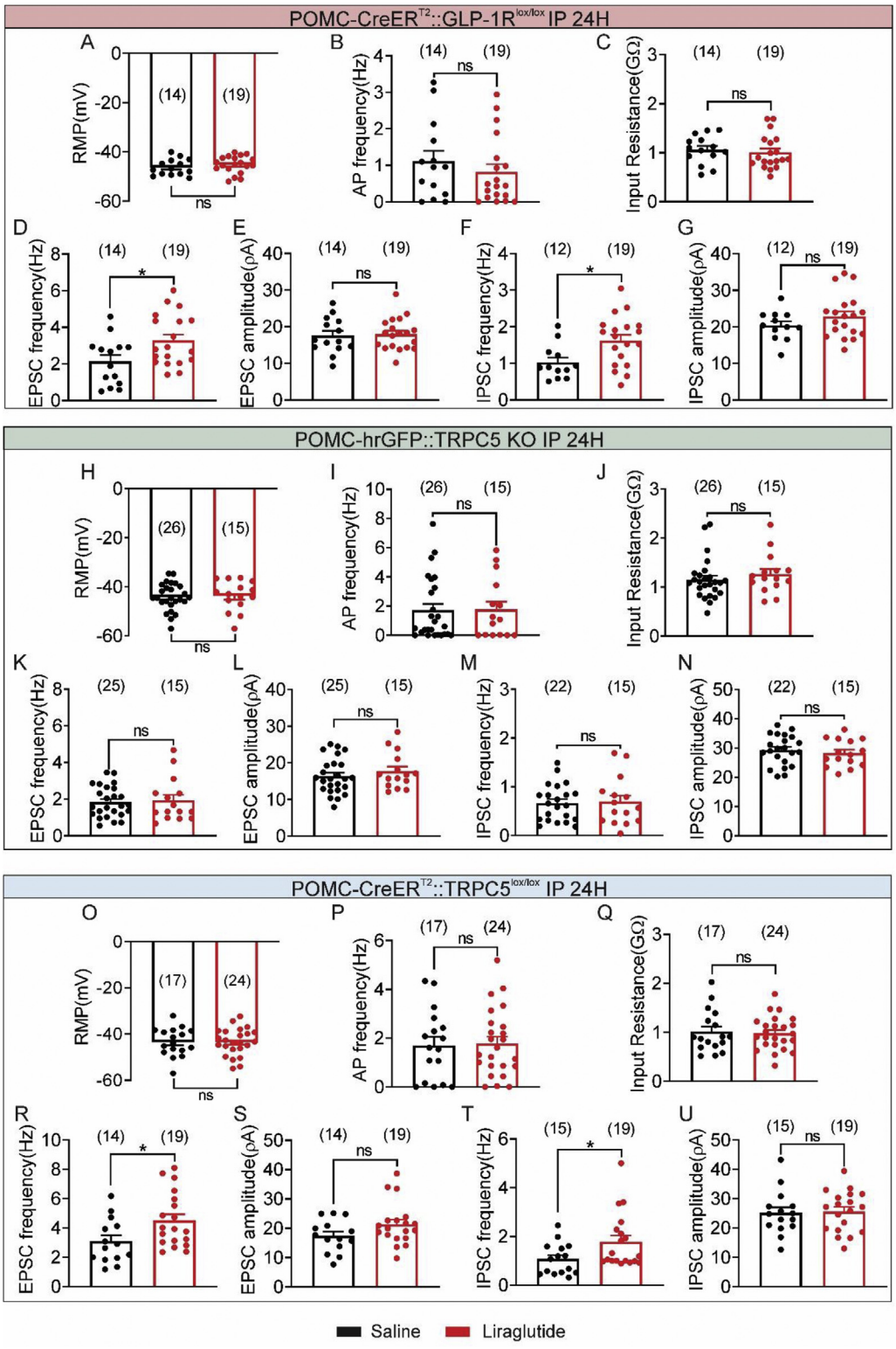


**Figure 5:** Liraglutide-induced activation of arcuate POMC neurons *in vivo* requires GLP-1 receptors and TRPC5 subunits in arcuate POMC neurons. (A–G) Histogram demonstrating the average resting membrane potential of POMC-hrGFP neurons (A), action potential frequency (B), input resistance (C), sEPSCs frequency (D), sEPSCs amplitude (E), sIPSCs frequency (F), sIPSCs amplitude (G) 24 h after injection of saline or liraglutide (300 μg/kg, I.P.) from mice deficient for GLP-1Rs in POMC neruons (POMC-CreERT2:GLP-1Rlox/lox:tdTomato mice). (H–N) Histogram demonstrating the average resting membrane potential of POMC-hrGFP neurons (H), action potential frequency (I), input resistance (J), sEPSCs frequency (K), sEPSCs amplitude (L), sIPSCs frequency (M), sIPSCs amplitude (N) 24 h after injection of saline or liraglutide (300 μg/kg, I.P.) from mice globally deficient for TRPC5 subunits (POMC-hrGFP:TRPC5 KO mice). (O–U) Histogram demonstrating the average resting membrane potential of POMC-hrGFP neurons (O), action potential frequency (P), input resistance (Q), sEPSCs frequency (R), sEPSCs amplitude (S), sIPSCs frequency (T), sIPSCs amplitude (U) 24 h after injection of saline or liraglutide (300 μg/kg, I.P.) from mice deficient for TRPC5 subunits in POMC neurons (POMC-Cre$^{ERT2}$:TRPC5$^{lox/lox}$:tdTomato mice). Data are from male mice and are expressed as mean ± SEM. *$p < 0.05$, unpaired t test compared to controls (black bar: saline; red bar: liraglutide). The number of neurons studied for each group is in parentheses.

 

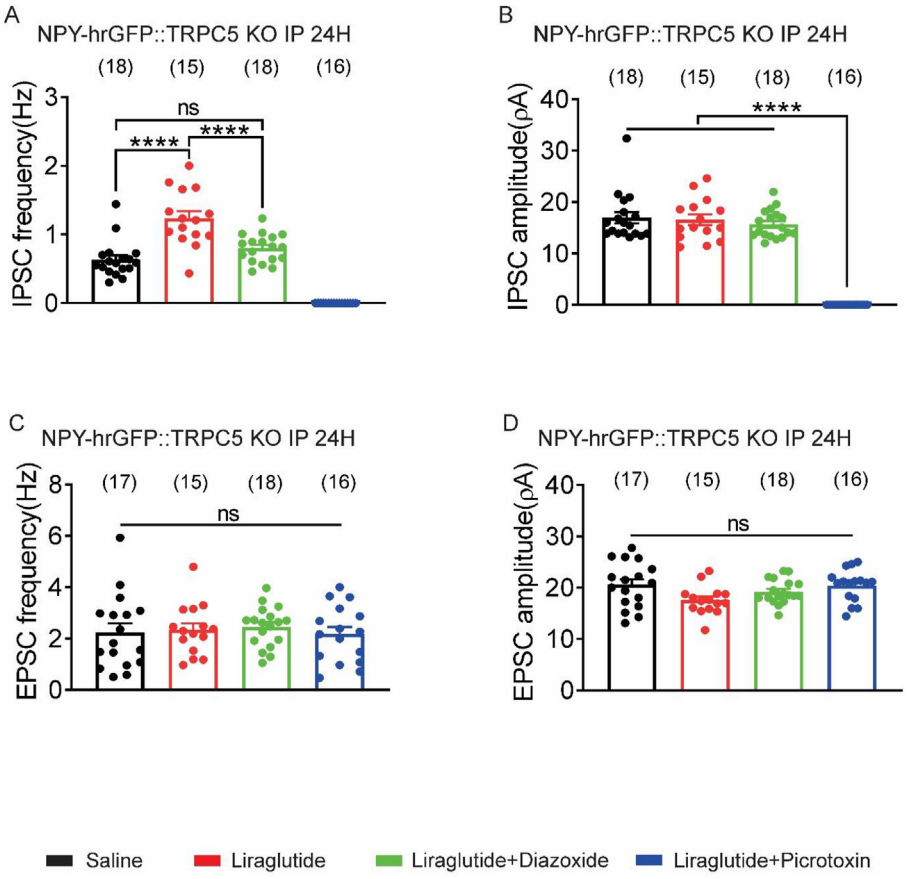


**Figure 6:** The Liraglutide-induced increase in inhibitory synaptic input to arcuate NPY neurons *in vivo* requires ATP-sensitive potassium channels (K-ATP) and TRPC5 subunits. (A—B) Histogram demonstrating the sIPSCs frequency (A) sIPSCs amplitude (B), sEPSC frequency (C), and sEPSC amplitude (D) of NPY neurons from of NPY-hrGFP:TRPC5 KO mice 24 h after injection of saline or liraglutide (300 μg/kg, I.P.). The Katp channel activator, diazoxide, or the GABA-A receptor antagonist, picrotoxin, was added to the recording chamber for some experiments (black bar: saline; red bar: liraglutide; green bar: liraglutide + diazoxide; blue bar: liraglutide + picrotoxin). Data are from male mice and are expressed as mean ± SEM and analyzed by two-way ANOVA with Tukey's post hoc test compared to controls, ****$p < 0.0001$. The number of neurons studied for each group is in parentheses.

targeted NPY neurons from mice globally deficient for TRPC5 subunits with the addition of a K-ATP channel agonist (diazoxide) in the recording chamber. Compared to mice injected with saline, the sIPSCs frequency and amplitude remained unchanged in mice injected with liraglutide ($p > 0.05$, $n = 18$; Figure 6 A-B, S7 A). These data suggest the GLP-1Ra induced increase in inhibitory input to NPY neurons *in vivo* requires both the activation of TRPC5 subunits and inhibition of KATP channels. We also examined the requirement of TRPC5 subunits and KATP channels in the GLP-1Ra induced decrease in excitatory input to NPY neurons. Global deficiency of TRPC5 subunits alone was sufficient to abrogate the decrease in excitatory synaptic input (Figure 6 C-D, S7 B). In particular, 24 h after injection of saline (I.P.), arcuate NPY neurons globally deficient for TRPC5 subunits had a sEPSCs frequency of 2.2 ± 0.4 Hz, n = 17 (Figure 6 C, S7 B). The frequency (sEPSCs = 2.3 ± 0.3 Hz, $p > 0.05$, $n = 15$, Figure 6 C, S7 B) and amplitude of sEPSCs remained unchanged 24 h after injection of liraglutide (I.P.) in NPY neurons globally deficient for TRPC5 subunits (Figure 6 D, S7 B). Similar results were observed while recording NPY neurons globally deficient for TRPC5 subunits in the presence of diazoxide, suggesting no additional role of KATP channels in this effect (sEPSCs = 2.5 ± 0.2Hz, $p > 0.05$, $n = 18$, Figure 6 C, S7 B).

Surprisingly, stimulation of TRPC5 subunits would be predicted to activate glutamatergic neurons resulting in an increased release of glutamate to postsynaptic (NPY/AgRP) neurons. Thus, we hypothesized that the GLP-1Ra dependent regulation of glutamatergic input may form a part of a polysynaptic circuit in which activation of GABAergic neurons may suppress excitatory input to NPY/AgRP neurons. In order to examine this, we targeted NPY neurons 2 h after chronic exposure to liraglutide with the addition of the GABA-A receptor antagonist, picrotoxin, in the recording chamber. The increase in excitatory synaptic input was abrogated in the presence of the GABA-A selective antagonist, picrotoxin (50 μM; sEPSCs = 3.1 ± 0.3 Hz, $p > 0.05$, $n = 16$; Figure S3 A—B). Importantly, picrotoxin alone failed to alter the RMP and action potential frequency of NPY neurons (50 μM; Figure S3 C—D). Together, these data support a GLP-1Ra dependent polysynaptic regulation of glutamatergic input to NPY neurons *in vivo*, which requires TRPC5 subunits and GABA-A receptors.

### 3.7. Liraglutide attenuates the AgRP neuron response to the sensory detection of food

To assess the effects of liraglutide on AgRP neuronal activity in awake and behaving animals, we next measured calcium dynamics in AgRP neurons as a proxy for neural activity. Based on our electrophysiological data, we hypothesized that GLP-1Ra's influence AgRP neuronal calcium dynamics in a time-dependent manner. Similar to previous reports [18,19] and the electrophysiological data presented in the

 

current study, liraglutide fails to alter the calcium levels of AgRP neurons within 30 min of liraglutide injection. However, as calcium dynamic measurements are not particularly well suited for longitudinal (i.e. 24 h) monitoring of neural activity, we next measured the ability of liraglutide to influence the change in AgRP neuron calcium dynamics in response to food. In food-deprived animals, AgRP neuronal calcium levels are rapidly suppressed in response to sensory detection and subsequent consumption of food [18,19,39–42]. This suppression of AgRP calcium levels in response to food predicts total food consumption, as the magnitude of this rapid sensory inhibition predicts the quantity of subsequent food intake [39,43]. Because liraglutide inhibits food intake, we hypothesized that liraglutide may abrogate the suppression of AgRP calcium levels that occurs in response to food presentation. Using fiber photometry, we measured calcium dynamics of AgRP neurons in food-restricted (85–90% body weight) animals in response to food presentation (Figure 7A,B) after injection of saline or liraglutide (300 μg/kg, I.P. at 2 h, 4 h, 12 h, and 24 h after injection of saline or liraglutide, timeline Figure 7C). As previously reported [18,19,39–42], food presentation rapidly inhibits AgRP neurons of mice injected with saline at all time points examined (Figure 7 and S8). We found that pretreatment with liraglutide markedly attenuated responses to food presentation at 2 and 4 h after liraglutide injection, but not at shorter (30 min) or longer (12 and 24 h) time points (Figure 7 D-F, S8 A-C).

Surprisingly, these data show suppression of liraglutide suppressed arcuate AgRP activity *in vivo* because liraglutide could not alter the membrane potential and the firing rate of NPY/AgRP neurons within 2 h in our electrophysiological recordings (Figure 3). However, the prior electrophysiological data were obtained from ad libitum-fed animals, while the in-vivo fiber photometry recordings were performed on food-restricted mice (85–90% body weight). To determine whether the nutritional state may influence the electrophysiological properties in response to liraglutide, whole-cell pCLAM recordings were performed in NPY neurons from food-restricted mice (85–90% body weight) 2 h after I.P. injection of saline or liraglutide (Figure 7G–J). Similar to previous reports, NPY neurons from food-restricted mice 2 h after injection with saline exhibited a depolarized membrane potential and an increase in action potential firing compared to ad libitum fed animals (food restriction – saline – 2 h: RMP = −37.4 ± 0.4 mV, APF = 4.8 ± 0.4 Hz, n = 10, Figure 7G–H). NPY neurons from food-restricted mice 2 h after injection with liraglutide (300 μg/kg, I.P.) were hyperpolarized, and they showed a decrease in action potential firing compared to saline treatment (food restriction – liraglutide – 2 h: RMP = −40.6 ± 1.5 mV, APF = 2.9 ± 0.6 Hz, n = 9, $p < 0.05$; Figure 7G–H). Notably, the absolute membrane potential reached in response to liraglutide was no different from that observed in ad libitum fed animals 2 h after liraglutide administration (Figure 3). Rather this effect was significant due to the more depolarized starting membrane potential and higher action potential frequency observed in response to food deprivation. Similar to the fiber photometry data, we did not observe this effect at longer time points, as the membrane potential and action potential firing of NPY neurons from food-restricted mice 24 h after injection with liraglutide (300 μg/kg, I.P.) was similar to saline controls (food restriction – saline – 24 h: RMP = −38.1 ± 1.4 mV, APF = 5.3 ± 0.8 Hz, n = 9; food restriction – liraglutide – 24 h: RMP = −37.1 ± 0.4 mV, APF = 4.2 ± 0.3 Hz, n = 10, $p > 0.05$; Figure 7G–H). The lack of a liraglutide-induced effect on NPY/AgRP activity 24 h after liraglutide injection in food-restricted mice may depend upon the altered nutrient state leading to an excitatory drive of NPY/AgRP neurons in these mice, which is further examined in the following section.

### 3.8. Metabolic state-dependent responsiveness of NPY/AgRP and POMC neurons to GLP-1R agonists

Activation of NPY/AgRP neurons in response to food deprivation is linked to an increase in excitatory input to arcuate NPY/AgRP neurons [44,45]. We hypothesized that the increased excitatory input that occurs during food deprivation may explain why liraglutide has more transient effects during extreme food deprivation. Indeed, NPY neurons from food-restricted mice (85–90% body weight) 2 and 24 h after injection with saline exhibited an increase in the frequency of excitatory input independent of changes in inhibitory input when compared to ad libitum fed animals (Figure 7I–J). NPY neurons from food-restricted mice 2 h after injection with liraglutide (300 μg/kg) exhibited an increase in inhibitory synaptic input concomitant with a decrease in excitatory synaptic activity (Figure 7I–J). This is notable as it is similar to what occurs 24 h after liraglutide injection in ad libitum fed animals (Figure 3). NPY neurons from food-restricted mice also showed an increase in inhibitory synaptic input 24 h after injection with liraglutide (Figure 7J). However, these neurons failed to show the decreased excitatory synaptic input previously observed at 2 h following liraglutide injection (Figure 7 I). Thus, food restriction drives an excitatory tone to NPY/AgRP neurons resulting in increased feeding behavior [44], which can be abrogated in early hours after liraglutide administration. However, the duration of the liraglutide-induced abrogation of excitatory input to NPY/AgRP neurons is short-lived in food-restricted animals when compared to ad libitum feeding.

To determine whether the effects of liraglutide administration are longer lasting in awake, behaving animals that are not food-deprived, we used fiber photometry. We measured calcium dynamics of AgRP neurons in response to food presentation 24 h after injection of either saline or liraglutide (300 μg/kg, I.P., Figure 8 A). While animals completely on an ad libitum chow diet failed to display a decrease in calcium levels in response to food presentation [18,19,39–42], we found that removing the food for 4 h was sufficient to observe a decrease of AgRP neuron activity in response to food drop (Figure 8 B, top). Importantly, under this moderate food withdrawal, liraglutide injected animals showed a markedly attenuated response to food presentation, even 24 h after liraglutide injection (Figure 8B–D). Together, these data offer a cellular basis for the temporally distinct liraglutide-induced changes in cellular activity, which depend upon the nutrient state.

In addition to nutrients, we recently demonstrated the plasticity of both arcuate POMC and NPY/AgRP neurons to exercise [34], resulting in an activity profile that is in agreement with beneficial effects on metabolism. Subsequent work suggests that these effects are observed in response to both forced and voluntary exercise [46]. Since their approval by the FDA in 2014, GLP-1R agonists are commonly prescribed either as a monotherapy or as an adjunct to exercise for blood glucose control as well as weight maintenance. Several reports suggest additive benefits of exercise and GLP-1R agonism on energy and glucose balance [47–50]. In particular, the combination of liraglutide and exercise decreased body weight and body fat percent twice as either strategy alone in obese individuals (BMI 32–43) who did not have diabetes for up to 1 year [48]. Also when combined subjects exhibited increased insulin sensitivity at the termination of the study [48]. This led to the hypothesis that exercise and GLP-1R agonism might be additive on the melanocortin circuit. We targeted arcuate POMC and NPY/AgRP neurons for electrophysiological recordings. To examine the combined effects of liraglutide and exercise, neurons were targeted 24 h after a single injection of liraglutide (300 μg/kg, I.P.). Prior to harvesting the brains, the mice also underwent a 1-hour HIIE exercise bout [34]. Liraglutide (300 μg/

 

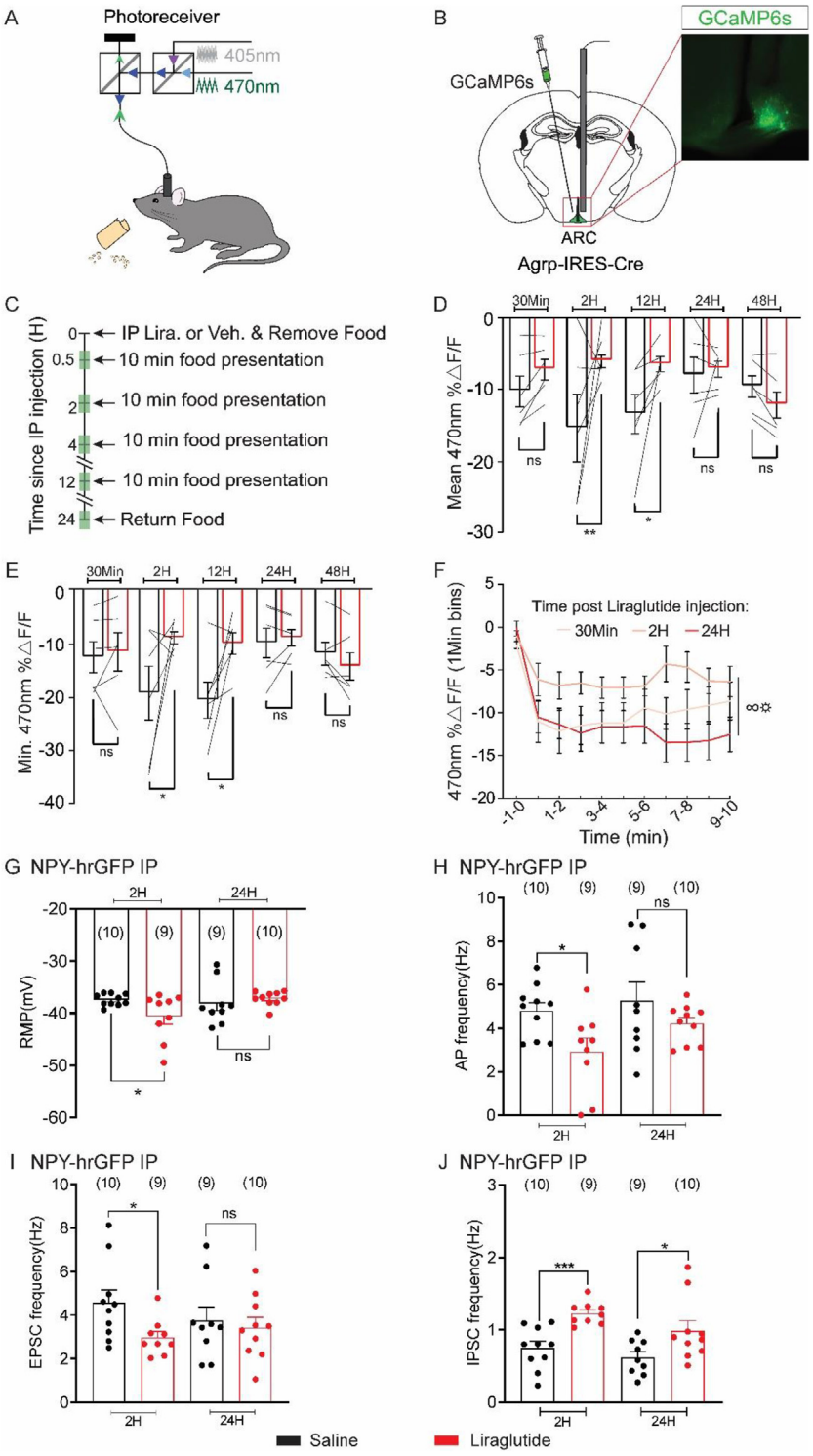


**Figure 7:** Liraglutide attenuates AgRP neuron activity changes in response to food in 24H food-deprived animals. (A) Schema depicting the fiber photometry system used to record calcium-dependent (470 nm) and independent (405 nm) fluorescence in awake, behaving mice. (B) Schematic and representative image showing GCaMP6s expression and fiber placement over AgRP neurons in the arcuate nucleus. Scale bar, 200 μm. (C) Timeline depicting experimental procedures. Shaded green areas represent fiber photometry recordings. (D) Mean ΔF/F of the 470 nm GCaMP6s signal following food presentation at various timepoints after vehicle or Liraglutide injection (see C). Thin black lines represent individual mice. Black, vehicle; red, Liraglutide ($n = 6$, two-way repeated-measures ANOVA, $^{*}p < 0.05$) (E) Minimum ΔF/F of the GCaMP6s signal following food presentation at various timepoints after vehicle or Liraglutide injection. Black, vehicle; red, Liraglutide ($n = 6$, two-way repeated-measures ANOVA, $^{*}p < 0.05$) (F) Mean ΔF/F (1 min bins) of the GCaMP6s signal following food presentation at various timepoints after Liraglutide injection ($n = 6$, two-way repeated-measures ANOVA, $p < 0.05$). (G-J) Histogram demonstrating the average resting membrane potential (G), action potential frequency (H), sEPSCs frequency (I), and sIPSCs frequency (J) of NPY-hrGFP neurons at 2 h and 24 h after injection with saline or liraglutide (black bar: saline; red bar: liraglutide, 300 μg/kg, I.P.). Data are expressed as mean ± SEM, ns $p > 0.05$, t-tests and post-hoc comparisons: $^{*}p < 0.05$, $^{**}p < 0.01$, $^{***}p < 0.001$. ANOVA interaction: $\infty p < 0.05$, ANOVA main effect of group: $\divideontimes p < 0.05$.

 

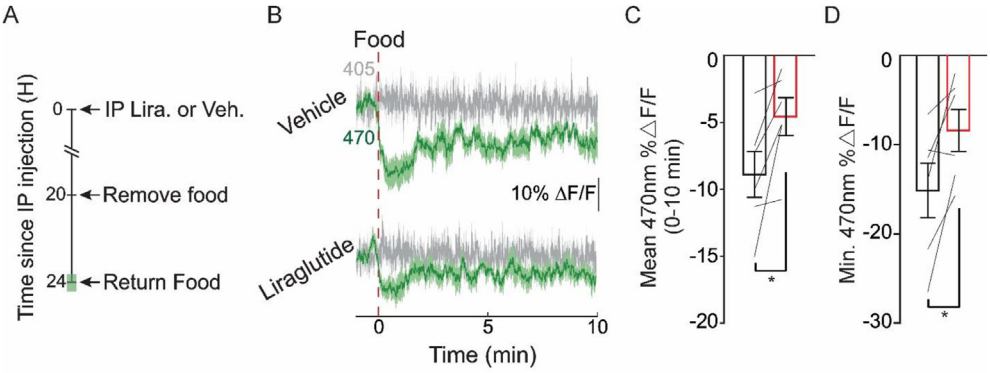


**Figure 8:** Long-term effects of Liraglutide on AgRP neurons during mild food deprivation. (A) Timeline depicting experimental procedure. The shaded green area represents fiber photometry recording. (B) Average ΔF/F of GCaMP6s signals during food presentation 24 h after I.P. injection of vehicle or liraglutide. Signals are aligned to food presentation (red dashed line). Green, 470 nm; grey, 405 nm. Dark lines represent means and lighter, shaded areas represent SEM. (C) Mean ΔF/F of the 470 nm GCaMP6s signals shown in (B). Thin black lines represent individual mice. Black, vehicle; red, Liraglutide ($n = 6$, paired t-test, $^*p < 0.05$). (D) Minimum ΔF/F of the 470 nm GCaMP6s signals shown in (B). Black, vehicle; red, Liraglutide ($n = 6$, paired t-test, $^*p < 0.05$). Data are expressed as mean ± SEM, t-tests: $^*p < 0.05$.

kg, I.P., 24 h prior) combined with exercise (1 h HIIE, immediately prior to recording) resulted in a larger depolarization of the resting membrane potential and sIPSCs frequency of arcuate POMC neurons when compared with the changes observed by liraglutide alone (300 μg/kg liraglutide + 1 h HIIE: RMP: −38.4 ± 1.2, n = 10, p = 0.05, APF: 4.8 ± 0.7, n = 10, p > 0.05, sEPSCs frequency: 3.8 ± 0.5, n = 10, p > 0.05, sIPSCs frequency: 1.9 ± 0.2, n = 10, p < 0.05, Figure S4 A—D). Similarly, liraglutide (300 μg/kg, I.P., 24 h prior) combined with exercise (1 h HIIE, immediately prior to recording) resulted in a larger hyperpolarization of arcuate NPY/AgRP neurons when compared with the changes observed of liraglutide alone (300 μg/kg liraglutide + 1 h HIIE: RMP: −48.8 ± 2.8, n = 10, $^*p < 0.05$, APF: 0.9 ± 0.3, n = 10, p = 0.05, sEPSCs: 1.4 ± 0.2, n = 10, p > 0.05, sIPSCs: 1.3 ± 0.2, n = 9, p > 0.05, Figure S4 E—H). Together these data demonstrate that GLP-1Ras alter the activity of POMC and NPY/AgRP neurons *in vivo* and that the temporal regulation by GLP-1Ras depends on the nutritional and metabolic state of the animal.

## 4. DISCUSSION

In the current study, we monitored the effect of both GLP-1Ras (liraglutide and semaglutide) *ex vivo* and *in vivo* on the activity of arcuate POMC and NPY/AgRP neuronal populations. Similar to previous reports on the acute effects of GLP-1Ras, the predominant effect of liraglutide and semaglutide on POMC activity was excitatory and inhibitory on NPY/AgRP neuronal activity. Importantly, these effects were not observed immediately after injection of GLP-1Ras; rather this occurred in a time-dependent manner that agrees with the pharmacokinetics of GLP-1Ras *in vivo* and varied depending on the nutrient state of the animal. Chronic exposure or injection of GLP-1Ras also recruited additional synaptic activity to arcuate POMC and NPY/AgRP neurons, not previously observed after acute administration. Moreover, we identified molecular mechanisms underlying these effects in POMC and NPY/AgRP neurons as well as altered activity of excitatory and inhibitory neurons that project to POMC and NPY/AgRP neurons. These effects in combination with those from previous work support a liraglutide and semaglutide dependent regulation of melanocortin neural circuitry with implications on energy balance and glucose metabolism.

### 4.1. Temporal regulation of cellular activity *in vivo* and *ex vivo*

Importantly, the GLP-1Ra induced alteration of NPY/AgRP cellular activity that occurs hours after injection was observed in both ex-vivo pCLAMP recordings as well as during *in vivo* fiber photometry measurements. This may appear at odds with previous work using fiber photometry, which demonstrated that GLP-1R agonists failed to alter the activity of arcuate NPY/AgRP neurons *in vivo* [18,19]. However, these studies only examined NPY/AgRP calcium dynamics within 30 min of injection [18,19]. This is notable because of the delayed pharmacokinetics of GLP-1Ras in rodents and humans [22,27,51]. In particular, serum liraglutide levels gradually rise following injection in humans, reaching a peak concentration within 8—12 h after injection [22,24,27], and similar time-to-peak concentrations (4—10 h) have been reported in rodents [23,51]. Moreover, injection of liraglutide (I.P. or S·C.) in rodents fails to significantly decrease food intake within 1 h of liraglutide injection [52]. Rather, the liraglutide dose-dependently decreases food intake 3—6 h after injection reaching a maximal suppression of food intake at 24 h [52]. In the current study, we examined the activity of NPY/AgRP neurons over hours to days after injection of GLP-1R agonists using patch-clamp electrophysiology and fiber photometry. In the patch-clamp studies performed on ad libitum fed animals, we found GLP-1R agonists altered the activity of both arcuate POMC and NPY/AgRP neurons in a time scale that agrees with the pharmacokinetic properties of GLP-1R agonists *in vivo*. While the activity of NPY/AgRP neurons was also altered in the fiber photometry experiments, we initially observed that this activity was accelerated compared to the patch-clamp experiments. There are several possible explanations for this discrepancy. First, the calcium dynamic changes that occur in response to food presentation reflect a sensory property of NPY/AgRP neurons. It implies that the changes observed in response to food presentation occur immediately at the presentation of food prior to consumption. The absolute magnitude and duration of this response thus depend on the consumption of a nutritive object. Thus the abrogation of the sensory detection of food may be an alteration of a circuit that projects to NPY/AgRP neurons which has yet to be identified and independent of the effects observed in the patch-clamp experiments. This may be an important technical consideration as NPY/AgRP neurons do not express GLP-1Rs. Rather presynaptic GABAergic neurons are required for liraglutide-induced changes in the NPY/AgRP activity [14,15]. Another possibility is that the fiber photometry results

 

might be a measure of activity, which is temporally dissociated from the patch-clamp experiments. In particular, the fiber photometry is likely measuring changes in cellular activity (using calcium levels as a proxy measure) in real-time, while the patch-clamp experiments may be detecting the plasticity of the circuit that occurs over many hours. Support for a GLP-1Ra dependent plasticity of this circuit may also come from the additional changes in the synaptic activity described in the current study, which has not been readily apparent with short acute administration of GLP-1Ras. In particular, we previously demonstrated that NPY/AgRP neurons receive more inhibitory input and POMC neurons more excitatory input following acute GLP-1Ra administration [14,15]. However, in the current study, chronic exposure or in-vivo injection of GLP-1Ras consistently increases inhibitory input to arcuate POMC neurons and decreases excitatory input to NPY/AgRP neurons as a population. Therefore, the activity changes that are seen in the fiber photometry experiments may initiate the plasticity that is detected in the later patch-clamp recordings. However, this assessment does not support the patch-clamp recordings that were performed in mice which were food restricted to a similar extent as the mice used in the fiber photometry experiments. After food restriction, the patch-clamp results mirrored the temporal changes that were observed in the fiber photometry experiments. Similarly, while ad libitum fed animals fail to demonstrate an AgRP induced suppression of calcium levels in response to chow food presentation, moderate (4 h) food deprivation was sufficient to elicit this activity. Importantly, the electrophysiological properties of NPY/AgRP neurons from 4 h food-restricted mice were similar to ad libitum fed animals. Moreover, suppression of AgRP calcium levels in response to food presentation of mice food-restricted for 4 h was abrogated 24 h after liraglutide injection, which matched the electrophysiological results from ad libitum fed animals. Thus, these data support consideration of activity changes in a context-dependent manner, depending upon the metabolic and/or nutrient state, and suggest a closer relationship between the fiber photometry and patch-clamp electrophysiological results than previously expected.

### 4.2. Cellular mechanisms of GLP-1Ra dependent activity in NPY/AgRP and POMC neurons

In a prior study, we demonstrated a GLP-1Ra dependent activation of arcuate POMC and inhibition of NPY/AgRP neurons [14–16]. However, these studies have largely relied on ex-vivo acute administration of GLP-1Ras to investigate this activity. Moreover, these ex-vivo assessments revealed changes in cellular activity in individual neurons which facilitated the description of both an activation and inhibition of arcuate NPY/AgRP and POMC neurons. Notably, the current study was an assessment of POMC or NPY/AgRP neuronal activity in response to chronic incubation or from mice that were injected with either saline or GLP-1Ras. Thus, we were not able to determine if each neuron acutely responded to GLP-1Ras. Rather the data presented are reflective of POMC and NPY/AgRP neuronal activity as a population. This is analogous to the changes in calcium levels observed in fiber photometry experiments. Together these data support a predominant activation of arcuate POMC and inhibition of arcuate NPY/AgRP in response to GLP-1Ras.

While POMC neurons express GLP-1Rs and the GLP-1Ra induced activation of arcuate POMC neurons persists in the presence of antagonists for action potentials and synaptic activity, the requirement of GLP-1Rs has not been directly assessed for this activity nor has the cellular activity of POMC neurons been examined in response to injection of GLP-1Ras. In the current study, we found that deficiency of GLP-1Rs in POMC neurons alone abrogated the depolarization and increased the firing rate of arcuate POMC neurons. Notably, the GLP-1Ra induced changes in excitatory; inhibitory synaptic activity to POMC neurons remained intact in POMC neurons deficient for GLP-1Rs. This suggests that while these synaptic inputs may alter transient changes in excitability, they may not contribute to the baseline membrane potential of arcuate POMC neurons. We also documented that GLP-1Ras failed to activate POMC neurons as well as change excitatory or inhibitory synaptic activity to POMC neurons in mice globally deficient for TRPC5 subunits. Moreover, GLP-1Ras failed to activate POMC neurons selectively deficient for TRPC5 subunits though changes in presynaptic activity remained intact. Together, both GLP-1Rs and TRPC5 subunits are critical for the GLP-1Ra dependent pre- and postsynaptic regulation of arcuate POMC activity.

In contrast to arcuate POMC neurons, arcuate NPY/AgRP neurons do not express GLP-1Rs [14,15,53]. We previously demonstrated that NPY/AgRP neurons are inhibited ex-vivo via an indirect upregulation of presynaptic GABA activity, which requires both TRPC5 subunits and KATP channels [14]. In the current study, injection of Liraglutide led to an increase in GABAergic synaptic activity to arcuate NPY/AgRP neurons on a similar time scale to effects observed in arcuate POMC neurons. However, in response to chronic administration or injection of GLP-1R agonists, NPY neurons also display a decrease in inhibitor input contributing to disinhibition of NPY neurons. Both the increase and inhibitory and decrease in excitatory input to NPY neurons were abrogated in mice globally deficient for TRPC5 subunits and pretreatment with KATP channel agonists. This suggests that Liraglutide inhibits NPY/AgRP neurons *in vivo* via presynaptic regulation of a TRPC5 and K-ATP channel-dependent mechanism.

Arcuate NPY/AgRP and POMC neurons receive inputs from a variety of brain nuclei [54–57]. Many of these input nuclei also express GLP-1Rs [58–69]. The current study shows that GLP-1Ras modify the synaptic input to both NPY/AgRP and POMC neurons. Importantly, we also show that at least in POMC neurons these inputs may not be sufficient to drive changes in RMP and APF of arcuate POMC neurons. However, the activity changes of NPY/AgRP neurons are entirely dependent upon this presynaptic regulation. In agreement with previous reports [14,15], the GLP-1Ra induced inhibition of NPY neurons requires presynaptic GABAergic neurons; however, it remains unclear where this neuron may reside in the brain. This warrants further investigation.

### 4.3. Physiological implications

Considerable effort has gone into defining the role of GLP-1Rs in the CNS to regulate energy balance and glucose metabolism. In particular, global deficiency of GLP-1Rs in mice attenuated the GLP-1 induced hypophagia while failing to alter body weight, suggesting that GLP-1Rs are not a key determinant of body mass under basal conditions [70]. Site-specific (either nucleus or cell type-specific) loss of function of GLP-1Rs in both mice and rats has led to a distributed network of neurons that are required in the brain for the GLP-1 dependent regulation of energy balance. With regard to arcuate POMC and NPY/AgRP neurons, GLP-1R antagonism within the arcuate nucleus abrogates the weight-reducing effects of Liraglutide [15]. Mice deficient in GLP-1Rs selectively display increased HFD-induced weight gain in POMC neurons independent of changes in food intake and energy expenditure [33]. Moreover, GLP-1R dependent activation of arcuate POMC neurons is required for the sustained reduction in body weight by the long-acting GLP-1R agonist, liraglutide [14]. As NPY/AgRP neurons do not express GLP-1Rs, less is known about the requirement of a GLP-1R dependent inhibition of arcuate NPY/AgRP neurons. The GLP-1R induced inhibition of NPY/AgRP neurons and abrogation of the sensory detection of food

 

observed in the current study would predict a decrease in food intake and suppress weight gain. However, it remains unclear whether this activity is required for GLP-1R dependent effects as glutamatergic neurons may be the primary cell type responsible for the Liraglutide-induced decrease in food intake and body weight [71]. However, GABAergic neurons may not be completely dispensable as inhibition of hindbrain GABAergic neurons attenuates the food intake and body weight-reducing effects of Liraglutide in rats on a high-fat diet [72]. Therefore, these data highlight the need to better understand the GLP-1R induced regulation of GABAergic signaling in energy homeostasis.

## 5. CONCLUSIONS

In summary, the long-acting GLP-1R agonists (liraglutide and semaglutide) activate arcuate POMC neurons while inhibiting arcuate NPY neurons *in vivo*. This activity is similar to the pharmacokinetics of GLP-1R agonist injection. In addition to the effects on POMC and NPY neuronal activity previously identified in acute ex-vivo studies, chronic exposure or in-vivo administration of GLP-1R agonists recruit additional synaptic regulation (i.e., decreased excitatory input to NPY neurons and increased inhibitory input to POMC neurons), both of which are dependent upon a GLP-1R agonist-induced excitation of upstream GABAergic neurons. The effects of GLP-1R agonists were also temporally dependent upon the nutritive state (ad libitum fed vs food-deprived) of the animal, and exercise enhanced the GLP-1R agonist-induced activity state of arcuate NPY and POMC neurons. This study reveals an underappreciated role for GLP-1 analogs to induce changes in cellular activity in the arcuate nucleus in-vivo and provides a physiological (i.e., exercise) and cellular mechanism by which this activity can be co-opted to enhance beneficial effects on energy balance and metabolism in the CNS.

## AUTHOR CONTRIBUTIONS

Y.D., J.C., N.G., Z.H., E—S. H., D.C., J.N·B., and K·W.W. designed the experiments. Y.D., J.C., N.G., Z.H., E—S. H., D.C., B·W., A.K. L.L., and Y.G. collected and analyzed the data. L.H. provided essential research tools. Y.D., J.C., Z.H., N.G., J.N·B., and K·W.W. wrote the manuscript. All authors reviewed and edited the manuscript. J.N.B. and K·W.W. are the guarantors of this work and thus had full access to all the data in the study and take responsibility for the integrity of the data and the accuracy of the data analysis.

## ACKNOWLEDGMENT

We thank Dr. Joel K. Elmquist (of the Division of Hypothalamic Research, Department of Internal Medicine, UT Southwestern Medical Center, Dallas, Texas) for providing us with the NPY-hrGFP and POMC-hrGFP mice. We also thank Dr. Randy J. Seeley (Department of Surgery, University of Michigan Health System, Ann Arbor, MI) for providing us with the GLP $1R^{lox/lox}$ mice. This work was supported by grants to K.W.W. (R01 DK100699, R01 DK119169, and P01 DK119130), J.N.B (R01 DK114104, ADA 118IBS116), E—S. H. (National Research Foundation of Korea — NRF 2021R1A6A3A14044733) and N.G. (National Science Foundation Graduate Research Fellowship Program DGE-1845298).

## CONFLICT OF INTEREST

No competing interests of any authors or persons related to this research are declared.

## APPENDIX A. SUPPLEMENTARY DATA

Supplementary data to this article can be found online at https://doi.org/10.1016/j.molmet.2021.101352.

## REFERENCES

[1] Kreymann, B., Williams, G., Ghatei, M.A., Bloom, S.R., 1987. Glucagon-like peptide-1 7-36: a physiological incretin in man. Lancet 2:1300—1304.
[2] Larsen, P.J., Tang-Christensen, M., Holst, J.J., Orskov, C., 1997. Distribution of glucagon-like peptide-1 and other preproglucagon-derived peptides in the rat hypothalamus and brainstem. Neuroscience 77:257—270.
[3] Mojsov, S., Weir, G.C., Habener, J.F., 1987. Insulinotropin: glucagon-like peptide I (7-37) co-encoded in the glucagon gene is a potent stimulator of insulin release in the perfused rat pancreas. Journal of Clinical Investigation 79:616—619.
[4] Drucker, D.J., 2018. Mechanisms of action and therapeutic application of glucagon-like peptide-1. Cell Metabolism 27:740—756.
[5] Holst, J.J., 2019. From the incretin concept and the discovery of GLP-1 to today's diabetes therapy. Frontiers in Endocrinology 10:260.
[6] Muller, T.D., Finan, B., Bloom, S.R., D'Alessio, D., Drucker, D.J., Flatt, P.R., et al., 2019. Glucagon-like peptide 1 (GLP-1). Mol Metab 30:72—130.
[7] Aponte, Y., Atasoy, D., Sternson, S.M., 2011. AGRP neurons are sufficient to orchestrate feeding behavior rapidly and without training. Nature Neuroscience 14:351—355.
[8] Steculorum, S.M., Ruud, J., Karakasilioti, I., Backes, H., Engstrom Ruud, L., Timper, K., et al., 2016. AgRP neurons control systemic insulin sensitivity via myostatin expression in Brown adipose tissue. Cell 165:125—138.
[9] Uner, A.G., Kecik, O., Quaresma, P.G.F., De Araujo, T.M., Lee, H., Li, W., et al., 2019. Role of POMC and AgRP neuronal activities on glycaemia in mice. Scientific Reports 9:13068.
[10] Zhan, C., Zhou, J., Feng, Q., Zhang, J.E., Lin, S., Bao, J., et al., 2013. Acute and long-term suppression of feeding behavior by POMC neurons in the brainstem and hypothalamus, respectively. Journal of Neuroscience: The Official Journal of the Society for Neuroscience 33:3624—3632.
[11] Cavalcanti-de-Albuquerque, J.P., Bober, J., Zimmer, M.R., Dietrich, M.O., 2019. Regulation of substrate utilization and adiposity by Agrp neurons. Nature Communications 10:311.
[12] Krashes, M.J., Koda, S., Ye, C., Rogan, S.C., Adams, A.C., Cusher, D.S., et al., 2011. Rapid, reversible activation of AgRP neurons drives feeding behavior in mice. Journal of Clinical Investigation 121:1424—1428.
[13] Gabery, S., Salinas, C.G., Paulsen, S.J., Ahnfelt-Ronne, J., Alanentalo, T., Baquero, A.F., et al., 2020. Semaglutide lowers body weight in rodents via distributed neural pathways. JCI Insight 5.
[14] He, Z., Gao, Y., Lieu, L., Afrin, S., Cao, J., Michael, N.J., et al., 2019. Direct and indirect effects of liraglutide on hypothalamic POMC and NPY/AgRP neurons - implications for energy balance and glucose control. Mol Metab 28:120—134.
[15] Secher, A., Jelsing, J., Baquero, A.F., Hecksher-Sorensen, J., Cowley, M.A., Dalboge, L.S., et al., 2014. The arcuate nucleus mediates GLP-1 receptor agonist liraglutide-dependent weight loss. Journal of Clinical Investigation 124:4473—4488.
[16] Peterfi, Z., Szilvasy-Szabo, A., Farkas, E., Ruska, Y., Pyke, C., Knudsen, L.B., et al., 2021. GLP-1 regulates the POMC neurons of the arcuate nucleus both directly and indirectly via presynaptic action. Neuroendocrinology 111:986—997.
[17] Ratner, C., He, Z., Grunddal, K.V., Skov, L.J., Hartmann, B., Zhang, F., et al., 2019. Long-acting neurotensin synergizes with liraglutide to reverse obesity through a melanocortin-dependent pathway. Diabetes 68:1329—1340.

 

[18] Beutler, L.R., Chen, Y., Ahn, J.S., Lin, Y.C., Essner, R.A., Knight, Z.A., 2017. Dynamics of gut-brain communication underlying hunger. Neuron 96:461–475 e465.

[19] Su, Z., Alhadeff, A.L., Betley, J.N., 2017. Nutritive, post-ingestive signals are the primary regulators of AgRP neuron activity. Cell Reports 21:2724–2736.

[20] Orskov, C., Wettergren, A., Holst, J.J., 1993. Biological effects and metabolic rates of glucagonlike peptide-1 7-36 amide and glucagonlike peptide-1 7-37 in healthy subjects are indistinguishable. Diabetes 42:658–661.

[21] Vilsboll, T., Agerso, H., Krarup, T., Holst, J.J., 2003. Similar elimination rates of glucagon-like peptide-1 in obese type 2 diabetic patients and healthy subjects. Journal of Clinical Endocrinology & Metabolism 88:220–224.

[22] Agerso, H., Jensen, L.B., Elbrond, B., Rolan, P., Zdravkovic, M., 2002. The pharmacokinetics, pharmacodynamics, safety and tolerability of NN2211, a new long-acting GLP-1 derivative, in healthy men. Diabetologia 45:195–202.

[23] Dong, S., Gu, Y., Wei, G., Si, D., Liu, C., 2018. Determination of liraglutide in rat plasma by a selective liquid chromatography-tandem mass spectrometry method: application to a pharmacokinetics study. Journal of chromatography. B, Analytical technologies in the biomedical and life sciences 1091:29–35.

[24] Jacobsen, L.V., Flint, A., Olsen, A.K., Ingwersen, S.H., 2016. Liraglutide in type 2 diabetes mellitus: clinical pharmacokinetics and pharmacodynamics. Clinical Pharmacokinetics 55:657–672.

[25] Jiang, J., Zhang, J., Jacobsen, L.V., Hu, P., 2011. The pharmacokinetics, pharmacodynamics, and tolerability of liraglutide, a once-daily human GLP-1 analogue, after multiple subcutaneous administration in healthy Chinese male subjects. The Journal of Clinical Pharmacology 51:1620–1627.

[26] Malm-Erjefalt, M., Bjornsdottir, I., Vanggaard, J., Helleberg, H., Larsen, U., Oosterhuis, B., et al., 2010. Metabolism and excretion of the once-daily human glucagon-like peptide-1 analog liraglutide in healthy male subjects and its in vitro degradation by dipeptidyl peptidase IV and neutral endopeptidase. Drug Metabolism & Disposition 38:1944–1953.

[27] Watson, E., Jonker, D.M., Jacobsen, L.V., Ingwersen, S.H., 2010. Population pharmacokinetics of liraglutide, a once-daily human glucagon-like peptide-1 analog, in healthy volunteers and subjects with type 2 diabetes, and comparison to twice-daily exenatide. The Journal of Clinical Pharmacology 50:886–894.

[28] Parton, L.E., Ye, C.P., Coppari, R., Enriori, P.J., Choi, B., Zhang, C.Y., et al., 2007. Glucose sensing by POMC neurons regulates glucose homeostasis and is impaired in obesity. Nature 449:228–232.

[29] van den Pol, A.N., Yao, Y., Fu, L.Y., Foo, K., Huang, H., Coppari, R., et al., 2009. Neuromedin B and gastrin-releasing peptide excite arcuate nucleus neuropeptide Y neurons in a novel transgenic mouse expressing strong Renilla green fluorescent protein in NPY neurons. J Neurosci 29:4622–4639.

[30] Gao, Y., Yao, T., Deng, Z., Sohn, J.W., Sun, J., Huang, Y., et al., 2017. TrpC5 mediates acute leptin and serotonin effects via pomc neurons. Cell Reports 18:583–592.

[31] Riccio, A., Li, Y., Moon, J., Kim, K.S., Smith, K.S., Rudolph, U., et al., 2009. Essential role for TRPC5 in amygdala function and fear-related behavior. Cell 137:761–772.

[32] Berglund, E.D., Liu, C., Sohn, J.W., Liu, T., Kim, M.H., Lee, C.E., et al., 2013. Serotonin 2C receptors in proopiomelanocortin neurons regulate energy and glucose homeostasis. Journal of Clinical Investigation 123:5061–5070.

[33] Burmeister, M.A., Ayala, J.E., Smouse, H., Landivar-Rocha, A., Brown, J.D., Drucker, D.J., et al., 2017. The hypothalamic glucagon-like peptide 1 receptor is sufficient but not necessary for the regulation of energy balance and glucose homeostasis in mice. Diabetes 66:372–384.

[34] He, Z., Gao, Y., Alhadeff, A.L., Castorena, C.M., Huang, Y., Lieu, L., et al., 2018. Cellular and synaptic reorganization of arcuate NPY/AgRP and POMC neurons after exercise. Mol Metab 18:107–119.

[35] He, Z., Lieu, L., Dong, Y., Afrin, S., Chau, D., Kabahizi, A., et al., 2021. PERK in POMC neurons connects celastrol with metabolism. JCI Insight 6.

[36] Sun, J., Gao, Y., Yao, T., Huang, Y., He, Z., Kong, X., et al., 2016. Adiponectin potentiates the acute effects of leptin in arcuate Pomc neurons. Mol Metab 5:882–891.

[37] Lieu, L., Chau, D., Afrin, S., Dong, Y., Alhadeff, A.L., Betley, J.N., et al., 2020. Effects of metabolic state on the regulation of melanocortin circuits. Physiology & Behavior 224:113039.

[38] Lerner, T.N., Shilyansky, C., Davidson, T.J., Evans, K.E., Beier, K.T., Zalocusky, K.A., et al., 2015. Intact-Brain Analyses Reveal Distinct Information Carried by SNc Dopamine Subcircuits. Cell 162:635–647.

[39] Beutler, L.R., Corpuz, T.V., Ahn, J.S., Kosar, S., Song, W., Chen, Y., et al., 2020. Obesity causes selective and long-lasting desensitization of AgRP neurons to dietary fat. eLife 9.

[40] Chen, Y., Lin, Y.C., Kuo, T.W., Knight, Z.A., 2015. Sensory detection of food rapidly modulates arcuate feeding circuits. Cell 160:829–841.

[41] Mandelblat-Cerf, Y., Ramesh, R.N., Burgess, C.R., Patella, P., Yang, Z., Lowell, B.B., et al., 2015. Arcuate hypothalamic AgRP and putative POMC neurons show opposite changes in spiking across multiple timescales. eLife 4.

[42] Mazzone, C.M., Liang-Guallpa, J., Li, C., Wolcott, N.S., Boone, M.H., Southern, M., et al., 2020. High-fat food biases hypothalamic and mesolimbic expression of consummatory drives. Nature Neuroscience 23:1253–1266.

[43] Goldstein, N., McKnight, A.D., Carty, J.R.E., Arnold, M., Betley, J.N., Alhadeff, A.L., 2021. Hypothalamic detection of macronutrients via multiple gut-brain pathways. Cell Metabolism 33:676–687 e675.

[44] Liu, T., Kong, D., Shah, B.P., Ye, C., Koda, S., Saunders, A., et al., 2012. Fasting activation of AgRP neurons requires NMDA receptors and involves spinogenesis and increased excitatory tone. Neuron 73:511–522.

[45] Takahashi, K.A., Cone, R.D., 2005. Fasting induces a large, leptin-dependent increase in the intrinsic action potential frequency of orexigenic arcuate nucleus neuropeptide Y/Agouti-related protein neurons. Endocrinology 146:1043–1047.

[46] Miletta, M.C., Iyilikci, O., Shanabrough, M., Sestan-Pesa, M., Cammisa, A., Zeiss, C.J., et al., 2020. AgRP neurons control compulsive exercise and survival in an activity-based anorexia model. Nat Metab 2:1204–1211.

[47] Ingelfinger, J.R., Rosen, C.J., 2021. STEP 1 for effective weight control - another first step? New England Journal of Medicine 384:1066–1067.

[48] Lundgren, J.R., Janus, C., Jensen, S.B.K., Juhl, C.R., Olsen, L.M., Christensen, R.M., et al., 2021. Healthy weight loss maintenance with exercise, liraglutide, or both combined. New England Journal of Medicine 384:1719–1730.

[49] Mensberg, P., Nyby, S., Jorgensen, P.G., Storgaard, H., Jensen, M.T., Sivertsen, J., et al., 2017. Near-normalization of glycaemic control with glucagon-like peptide-1 receptor agonist treatment combined with exercise in patients with type 2 diabetes. Diabetes, Obesity and Metabolism 19:172–180.

[50] Wilding, J.P.H., Batterham, R.L., Calanna, S., Davies, M., Van Gaal, L.F., Lingvay, I., et al., 2021. Once-weekly semaglutide in adults with overweight or obesity. New England Journal of Medicine 384:989.

[51] P.a.M.D.A., 2009. Report on deliberation results - victoza subcutaneous injection 18mg. p. 119. Liraglutide.

[52] Hayes, M.R., Kanoski, S.E., Alhadeff, A.L., Grill, H.J., 2011. Comparative effects of the long-acting GLP-1 receptor ligands, liraglutide and exendin-4, on food intake and body weight suppression in rats. Obesity 19:1342–1349.

[53] Biglari, N., Gaziano, I., Schumacher, J., Radermacher, J., Paeger, L., Klemm, P., et al., 2021. Functionally distinct POMC-expressing neuron subpopulations in hypothalamus revealed by intersectional targeting. Nature Neuroscience 24:913–929.

[54] Garfield, A.S., Li, C., Madara, J.C., Shah, B.P., Webber, E., Steger, J.S., et al., 2015. A neural basis for melanocortin-4 receptor-regulated appetite. Nature Neuroscience 18:863–871.

 

[55] Krashes, M.J., Shah, B.P., Madara, J.C., Olson, D.P., Strochlic, D.E., Garfield, A.S., et al., 2014. An excitatory paraventricular nucleus to AgRP neuron circuit that drives hunger. Nature 507:238—242.

[56] Ryan, P.J., Ross, S.I., Campos, C.A., Derkach, V.A., Palmiter, R.D., 2017. Oxytocin-receptor-expressing neurons in the parabrachial nucleus regulate fluid intake. Nature Neuroscience 20:1722—1733.

[57] Sutton, A.K., Gonzalez, I.E., Sadagurski, M., Rajala, M., Lu, C., Allison, M.B., et al., 2020. Paraventricular, subparaventricular and periventricular hypothalamic IRS4-expressing neurons are required for normal energy balance. Scientific Reports 10:5546.

[58] Alhadeff, A.L., Baird, J.P., Swick, J.C., Hayes, M.R., Grill, H.J., 2014. Glucagon-like Peptide-1 receptor signaling in the lateral parabrachial nucleus contributes to the control of food intake and motivation to feed. Neuropsychopharmacology: official publication of the American College of Neuropsychopharmacology vol. 39:2233—2243.

[59] Brierley, D.I., Holt, M.K., Singh, A., de Araujo, A., Vergara, M., Afaghani, M.H., et al., 2020. Central and peripheral GLP-1 systems independently and additively suppress eating. bioRxiv vol. 2008:234427.

[60] Campos, R.V., Lee, Y.C., Drucker, D.J., 1994. Divergent tissue-specific and developmental expression of receptors for glucagon and glucagon-like peptide-1 in the mouse. Endocrinology 134:2156—2164.

[61] Hoosein, N.M., Gurd, R.S., 1984. Human glucagon-like peptides 1 and 2 activate rat brain adenylate cyclase. FEBS Letters 178:83—86.

[62] Kabahizi, A., Wallace, B., Lieu, L., Chau, D., Dong, Y., Hwang, E.S., et al., 2021. Glucagon-like peptide-1 (GLP-1) signaling in the brain: from neural circuits and metabolism to therapeutics. British Journal of Pharmacology.. https://pubmed.ncbi.nlm.nih.gov/34519026/https://bpspubs.onlinelibrary.wiley.com/doi/10.1111/bph.15682.

[63] Kanoski, S.E., Fortin, S.M., Arnold, M., Grill, H.J., Hayes, M.R., 2011. Peripheral and central GLP-1 receptor populations mediate the anorectic effects of peripherally administered GLP-1 receptor agonists, liraglutide and exendin-4. Endocrinology 152:3103—3112.

[64] Kanoski, S.E., Hayes, M.R., Skibicka, K.P., 2016. GLP-1 and weight loss: unraveling the diverse neural circuitry. American Journal of Physiology - Regulatory, Integrative and Comparative Physiology 310:R885—R895.

[65] Kanse, S.M., Kreymann, B., Ghatei, M.A., Bloom, S.R., 1988. Identification and characterization of glucagon-like peptide-1 7-36 amide-binding sites in the rat brain and lung. FEBS Letters 241:209—212.

[66] Sandoval, D.A., Bagnol, D., Woods, S.C., D'Alessio, D.A., Seeley, R.J., 2008. Arcuate glucagon-like peptide 1 receptors regulate glucose homeostasis but not food intake. Diabetes 57:2046—2054.

[67] Vahl, T.P., Tauchi, M., Durler, T.S., Elfers, E.E., Fernandes, T.M., Bitner, R.D., et al., 2007. Glucagon-like peptide-1 (GLP-1) receptors expressed on nerve terminals in the portal vein mediate the effects of endogenous GLP-1 on glucose tolerance in rats. Endocrinology 148:4965—4973.

[68] Wei, Y., Mojsov, S., 1995. Tissue-specific expression of the human receptor for glucagon-like peptide-I: brain, heart and pancreatic forms have the same deduced amino acid sequences. FEBS Letters 358:219—224.

[69] Yamamoto, H., Kishi, T., Lee, C.E., Choi, B.J., Fang, H., Hollenberg, A.N., et al., 2003. Glucagon-like peptide-1-responsive catecholamine neurons in the area postrema link peripheral glucagon-like peptide-1 with central autonomic control sites. Journal of Neuroscience 23:2939—2946.

[70] Scrocchi, L.A., Brown, T.J., MaClusky, N., Brubaker, P.L., Auerbach, A.B., Joyner, A.L., et al., 1996. Glucose intolerance but normal satiety in mice with a null mutation in the glucagon-like peptide 1 receptor gene. Natura Med 2:1254—1258.

[71] Adams, J.M., Pei, H., Sandoval, D.A., Seeley, R.J., Chang, R.B., Liberles, S.D., et al., 2018. Liraglutide modulates appetite and body weight through glucagon-like peptide 1 receptor-expressing glutamatergic neurons. Diabetes 67:1538—1548.

[72] Fortin, S.M., Lipsky, R.K., Lhamo, R., Chen, J., Kim, E., Borner, T., et al., 2020. GABA neurons in the nucleus tractus solitarius express GLP-1 receptors and mediate anorectic effects of liraglutide in rats. Science Translational Medicine 12.

 